chemosensors

MDPI

Review

Advanced GC-MS Chemosensing Combined with Atomistic Modeling: A Synergistic Approach for Environmental Water Analysis

Sanja J. Armaković [1] and Stevan Armaković [2,*]

[1] Department of Chemistry, Biochemistry and Environmental Protection, Faculty of Sciences, University of Novi Sad, 21000 Novi Sad, Serbia; sanja.armakovic@dh.uns.ac.rs
[2] Department of Physics, Faculty of Sciences, University of Novi Sad, 21000 Novi Sad, Serbia
* Correspondence: stevan.armakovic@df.uns.ac.rs

Abstract

Gas chromatography–mass spectrometry (GC-MS) plays a crucial role in analyzing complex water samples due to its high sensitivity, selectivity, and robustness. Recent developments have transformed GC-MS into a powerful chemosensor platform, capable of generating detailed chemical fingerprints for targeted or untargeted environmental analysis. This review highlights the integration of GC-MS with atomistic modeling approaches, including quantum chemical calculations and molecular simulations, to enhance the interpretation of mass spectra and support the identification of emerging contaminants and transformation products. These computational tools offer mechanistic insight into fragmentation pathways, molecular reactivity, and pollutant behavior in aqueous environments. Emphasis is placed on recent trends that couple GC-MS with machine learning, advanced sample preparation, and simulation-based spectrum prediction, forming a synergistic analytical framework for advanced water contaminant profiling. The review concludes by addressing current challenges and outlining future perspectives in combining experimental and theoretical tools for intelligent environmental monitoring.

Keywords: environmental contaminants; non-targeted analysis; mass spectral interpretation; atomistic calculations; molecular dynamics; predictive environmental modeling

Received: 29 June 2025
Revised: 8 September 2025
Accepted: 16 September 2025
Published: 19 September 2025

Citation: Armaković, S.J.; Armaković, S. Advanced GC-MS Chemosensing Combined with Atomistic Modeling: A Synergistic Approach for Environmental Water Analysis. *Chemosensors* **2025**, *13*, 353. https://doi.org/10.3390/chemosensors13090353

1. Introduction

Chemosensing is the process of detecting and interpreting chemical signals, and has become a central concept in modern environmental analysis [1,2]. While the term is often associated with chemical sensors, advanced analytical platforms such as gas chromatography–mass spectrometry (GC-MS) can also be regarded as chemosensing tools, since they generate characteristic fingerprints that enable the detection and interpretation of environmental contaminants. When it comes to water quality monitoring, chemosensing extends beyond single-target analysis toward the recognition of complex chemical patterns that reflect contaminants, their transformation products, and interactions with natural matrices [1,3–5].

Emerging contaminants (ECs), including pharmaceuticals, products for personal care, pesticides, and industrial chemicals, represent a threat of growing concern to ecosystems and human health due to their persistence, bioaccumulation potential, and toxicology. Addressing these challenges requires advanced analytical tools capable of detecting and quantifying trace levels of ECs in complex environmental matrices [6–10].

This review highlights the critical role of mass spectrometry (MS) in monitoring ECs, focusing attention on high sensitivity, specificity, and adaptability across various techniques such as GC-MS. The application of MS has enabled the real-time detection of volatile organic compounds (VOCs), the comprehensive non-targeted screening of unknown contaminants, and the correct quantification of compounds in different matrices [1,11–14]. While other MS techniques, including liquid chromatography–mass spectrometry and high-resolution mass spectrometry, have also made significant contributions to environmental analysis, the primary focus of this review is on the application of GC-MS as the dominant tool for monitoring ECs.

Despite its efficacy, challenges such as matrix interferences, a lack of standardized methodologies, and limited spectral libraries persist [1,15]. Recent advancements in the form of hybrid MS systems, the application of atomistic calculations, and the usage of artificial intelligence (AI), generate opportunities for more efficient environmental monitoring and predictive modeling of contaminant behavior [2,16,17]. Improvements in MS technologies and collaborative efforts are essential to overcome existing challenges and ensure sustainable solutions for dealing with the risks associated with emerging contaminants.

GC-MS has long been a foundational technique in environmental chemistry, recognized for its ability to separate, identify, and quantify volatile and semi-volatile compounds. Initially developed for petroleum and industrial applications in the mid-20th century, GC-MS was rapidly adopted for environmental monitoring with the rise in global concern over persistent organic pollutants (POPs), chlorinated pesticides, and hazardous industrial chemicals [11,12]. In its early usage, GC-MS was primarily applied in targeted analysis, where the identity and behavior of analytes were known, and the focus was on quantification using standard reference compounds.

Due to the growing complexity of environmental samples and the emergence of contaminants of emerging concern (CECs), often unknown, unregulated, or present at trace levels, analytical methods must be improved over time. In response, GC-MS evolved into a powerful chemosensing platform capable of delivering both targeted and non-targeted insights [13,15,18,19]. Modern approaches utilize the total ion chromatogram (TIC) and total ion mass spectrum (TIMS) not only for compound identification but also as holistic chemical signatures of the sample. These rich datasets are often interpreted using multivariate statistics and machine learning (ML) algorithms, enabling the classification of water samples based on pollution patterns even in the absence of individual analyte identification.

Technological advancements further accelerated this transition. The integration of high-resolution time-of-flight mass spectrometry (HR–ToFMS) and comprehensive two-dimensional gas chromatography (GC×GC) has significantly enhanced sensitivity, selectivity, and dynamic range, enabling the detection of trace-level pollutants and their isomers in highly complex water matrices [1,17,19,20].

GC×GC has emerged as a leading technique for resolving co-eluting compounds and revealing the chemical diversity of environmental samples. These improvements have broadened the application of GC-MS from routine water testing to advanced exposome studies, source tracking, and forensic environmental analysis [10,16,21,22].

Portable and miniaturized GC-MS instruments are being introduced for in situ and real-time environmental monitoring, addressing the demand for rapid field-based assessments. Complemented by cloud-based databases and AI-driven processing tools, these platforms are poised to support decentralized water quality surveillance networks [1,16,17].

In environmental science, GC-MS has moved from measuring one pollutant at a time to using smarter, more integrated chemosensing approaches. This transformation is critical

for managing the increasingly complex mix of aquatic contaminants and for ensuring sustainable water resource management in an era of emerging pollutants.

The development of gas GC-MS has moved far beyond its original role in targeted pollutant detection [11,12,16]. Traditionally used to quantify known analytes through reference standards, GC-MS is now evolving into a tool for intelligent environmental diagnostics [1,17]. This transformation is driven by the need to manage complex mixtures of known and unknown contaminants, particularly in the context of emerging pollutants and dynamic environmental systems [2,6,15].

Modern GC-MS systems, often combined with high-resolution platforms (e.g., GC×GC–ToFMS) and integrated with chemometric and ML tools, enable the interpretation of comprehensive chemical fingerprints [2,18–20]. These intelligent systems can classify water quality, trace pollution sources, and even predict contaminant behavior without prior knowledge of analyte identity [1,17,18]. This shift from simple detection to data-rich diagnostics represents an important change in environmental monitoring, aligning analytical chemistry with the goals of sustainability, risk prediction, and real-time decision-making [1,10,23].

This review aims to highlight recent advances in GC-MS chemosensing for environmental applications. It emphasizes the shift from traditional targeted detection to intelligent diagnostics supported by high-resolution instrumentation, multivariate statistics, and ML. In addition to these data-driven approaches, we underscore the growing importance of atomistic calculations and computational chemistry tools that enable predictive modeling of molecular fragmentation and enhance the interpretation of mass spectra. The structure of this review covers GC-MS fundamentals, technological innovations such as GC×GC and portable systems, modern data-analytical methods, and practical applications for monitoring emerging contaminants. The novelty of this review lies in its integrated perspective, combining analytical chemistry with advanced atomistic simulations and computational workflows to present GC-MS as a comprehensive, versatile, and predictive platform for environmental monitoring.

2. GC-MS as a Chemosensing Platform for Environmental Analysis

This section introduces the foundational principles of GC-MS and explores how this traditional analytical platform has evolved into an advanced chemosensing system for environmental monitoring.

GC-MS is an analytical technique that combines the high-efficiency separation GC with the molecular identification and quantification capabilities of MS. In GC, analytes are vaporized and transported through a capillary column by an inert carrier gas (typically helium or nitrogen), where separation occurs based on differences in volatility and affinity toward the stationary phase (Figure 1). This process yields temporally resolved elution profiles, enabling the deconvolution of complex mixtures into their components [11,12,21].

The eluted compounds then enter the MS detector, where they are ionized, most commonly through electron ionization (EI) or chemical ionization (CI). EI provides consistent and reproducible fragmentation patterns that facilitate structural elucidation and database matching, whereas CI generates molecular ions with minimal fragmentation, aiding in molecular weight determination [11,12]. Ions are separated according to their mass-to-charge (m/z) ratios using mass analyzers such as quadrupoles, ion traps, or time-of-flight (ToF) systems. The resulting spectra serve as chemical fingerprints, enabling the identification and quantification of target and non-target compounds [1,11,16].

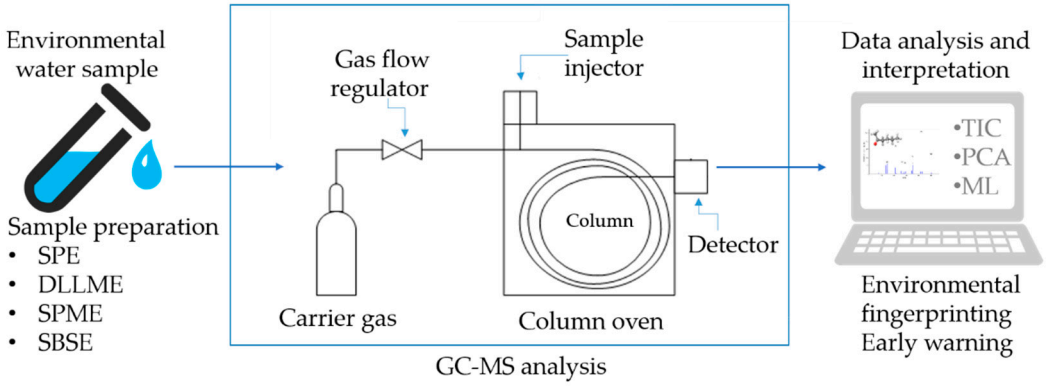

Figure 1. Overview of GC-MS workflow for environmental chemosensing.

GC-MS has become a foundational tool in environmental and water quality monitoring due to its robustness, high sensitivity, and applicability to a broad range of volatile and semi-volatile organic pollutants [19,21]. The technique's integration with extensive mass spectral libraries and advanced data processing platforms continues to expand its role in both regulatory and exploratory environmental analyses [15,19].

2.1. Principles and Evolution of Chemosensing in Environmental Applications

Chemosensing in environmental analysis refers to the detection, interpretation, and classification of chemical information from complex samples by translating molecular-level interactions into measurable signals. Unlike traditional targeted analysis, which focuses on the quantification of specific known analytes, chemosensing adopts a broader systems-level approach. Within this framework, the concept of a chemical "fingerprint" is used to describe the characteristic patterns obtained from analytical measurements [1,24]. These fingerprints reflect not only the presence of individual contaminants but also their transformation products and interactions with the natural matrix, such as organic matter, sediments, or biological components [21].

Environmental fingerprints are thus constructed from complex datasets generated by advanced techniques such as GC-MS and comprehensive two-dimensional GC (GC×GC-MS). For instance, Acharya et al. [21] used GC-MS to profile VOCs in aquatic matrices, demonstrating how VOC patterns could be linked to specific contamination sources and environmental behaviors. Similarly, Jia et al. [15] employed non-target screening (NTS) to compare fingerprints across laboratories and instrument setups, highlighting reproducibility issues and the need for harmonized workflows.

Chemosensing not only accounts for the parent pollutants but also captures secondary transformation products, metabolites, and interactions with natural matrices, such as dissolved organic matter, sediments, or microbial communities. For example, in complex river water analysis, Schreiber et al. [10] demonstrated how environmental fingerprints could reflect the presence of Watch List substances in both water and microplastics, offering a broader picture of contaminant fate and transport.

Recent advancements in chemometrics and ML have further enhanced the interpretation of these fingerprints. Multivariate tools, such as principal component analysis (PCA) and partial least squares–discriminant analysis (PLS-DA), enable researchers to extract latent patterns, classify water types, and associate contaminant profiles with anthropogenic sources or natural gradients [2,16]. AI-driven methods are increasingly integrated into GC-MS workflows, from tensor-based modeling approaches that automate reproducible peak table generation to convolutional neural networks that enable robust classification of complex chemical signatures such as ignitable liquids in fire debris [25,26]. These advanced

analytical tools illustrate how chemosensing is evolving into a comprehensive approach to environmental monitoring.

Importantly, chemosensing is not limited to compound detection but extends to source tracking, ecological risk prediction, and exposome profiling, thereby providing a multidimensional understanding of environmental quality. This approach is especially crucial when dealing with CECs, such as pharmaceuticals, personal care products, flame retardants, or microplastics (and their nano counterparts), which often exist at trace levels and exhibit complex environmental behavior [6,27].

Central to chemosensing is the concept of chemical signal recognition, a process that begins with the detection of changes in physical or chemical properties that arise from complex mixtures. These signals often manifest as shifts in retention time, changes in mass spectral fragmentation patterns, variations in ion intensity, or alterations in compound elution behavior. For instance, in the GC-MS-based analysis of different waters contaminated with pharmaceuticals and pesticides, characteristic ion signatures can signal not only the presence of parent compounds but also their degradation intermediates or matrix-bound forms [13,28].

Following signal detection, pattern recognition becomes crucial for interpreting high-dimensional data. This is typically achieved using chemometric techniques, such as PCA, PLS-DA, and Hierarchical Cluster Analysis (HCA) [24]. These multivariate tools reduce data dimensionality while preserving variance, allowing researchers to classify water samples, group contamination profiles, and identify pollution sources based on their chemical fingerprints. Vosough et al. [1] applied PCA to distinguish between water samples impacted by agricultural runoff and those affected by urban wastewater. A recent study demonstrated how GC-MS based technique combined with a two-step chemometric workflow, including PCA and PLS-DA, can effectively discriminate wine varieties and identify characteristic chemical markers, achieving high classification accuracy [29].

Increasingly, ML models such as Support Vector Machine (SVM), Random Forest (RF), and neural networks are being used to enhance classification performance and support automated feature extraction. Recent studies have demonstrated that coupling GC–MS with machine learning enables diverse applications, including the classification of novel psychoactive substances [30], the authentication and geographic tracing of medicinal plants such as Artemisia argyi [31], and the robust differentiation of botanical sources, regions, and production modes of Atractylodes species [32], thereby enhancing both analytical accuracy and quality control. Additionally, Houhou et al. [2] demonstrated the utility of unsupervised ML methods for identifying previously unknown patterns of pollutants.

This pattern recognition workflow transforms GC-MS from a conventional detection tool into an intelligent chemosensing platform, capable of revealing not only the presence of contaminants but also broader trends related to ecosystem health, pollution origin, and temporal changes in environmental pressure. As the complexity of environmental matrices continues to increase, the role of advanced pattern recognition in chemosensing is expected to become increasingly central to environmental monitoring and regulatory frameworks [1,2,15,16,33].

The resulting environmental fingerprints, a composite of chromatographic retention patterns and mass spectral features, act as diagnostic markers for assessing water quality. These fingerprints reflect not only the presence of target pollutants but also encompass transformation products, matrix interactions, and unidentified co-contaminants. This richness of data is particularly valuable in NTS workflows, where prior knowledge of analyte identity is not required. When interpreted using advanced data processing pipelines, including unsupervised and supervised ML algorithms (e.g., PCA, HCA, PLS-DA, RF),

these complex datasets facilitate robust source tracking, early warning detection, and exposure characterization [1,2].

Such algorithmic interpretation transforms GC-MS from a traditional instrument into a systems-level chemosensing platform, capable of recognizing subtle shifts in chemical composition that signal anthropogenic impacts, seasonal variations, or ecological disturbances. These tools have been increasingly applied in water surveillance, sediment analysis, and pollution source attribution, often in real-time or near-real-time monitoring systems [1,2,16,19,22,33].

To further illustrate these principles, the following section presents an overview of core chemosensing concepts as applied in GC-MS-based environmental analysis. Table 1 categorizes the major chemosensing elements that underpin GC-MS-based environmental monitoring and illustrates how each contributes to data interpretation, contaminant detection, and ecosystem assessment.

Table 1. Key concepts and functional roles of chemosensing in environmental GC-MS applications.

Concept	Key Features	Functional Role	Ref.
Signal recognition and processing	Detection of molecular-level responses (e.g., retention time shifts, mass spectra changes)	Enables identification of known/unknown analytes and structural elucidation	[1,12,34,35]
Pattern recognition	Use of PCA, PLS–DA, clustering, and AI/ML to recognize trends	Discriminates between sample types, pollution sources, and contamination events	[24,36,37]
Environmental fingerprinting	Total ion chromatograms and full-scan spectra representing the whole sample	Provides a holistic chemical profile for classification, source tracking, and pollution assessment	[38,39]
Non-Target Screening (NTS)	Data-rich acquisition without predefined target compounds	Discovery of novel and emerging contaminants	[40–43]
Real-time monitoring	Miniaturized GC-MS devices, sensor integration, and remote sensing	Field-based, rapid decision support for environmental safety	[44–46]

Yang et al. [47] demonstrated how total ion current profiles obtained by DLLME–GC-MS for non-targeted screening of VOC in drinking water, highlighting their potential for differentiating contamination patterns. Duff et al. [16] demonstrated the use of portable GC-MS for in-field screening of organic pollutants in soil and water at pollution incidents, highlighting its potential for rapid environmental assessments relevant to agricultural contamination scenarios.

Each concept listed in Table 1 illustrates a critical component of how chemosensing has evolved within GC-MS environmental analysis. Together, they provide a robust analytical framework for interpreting complex datasets and making informed decisions about ecosystem health and pollutant behavior.

While traditionally qualitative in focus, these developments have laid the groundwork for a transition toward quantitative chemosensing, as discussed in the following section.

2.2. Transition from Qualitative to Quantitative Chemosensing

The evolution of chemosensing in GC-MS has progressed beyond the mere qualitative detection of contaminants to more advanced, quantitative aspects. GC-MS applications in environmental monitoring primarily focus on identifying the presence or absence of specific compounds, often by relying on characteristic ion fragments or retention times. While this

approach remains foundational, it is increasingly complemented by quantitative strategies that allow for the modeling, prediction, and real-time assessment of environmental dynamics. This evolution is evident in large-scale environmental monitoring campaigns, where GC-MS data, integrated with predictive models, have enabled the dynamic assessment of pollutant behavior in aquatic ecosystems [18,27,33].

Quantitative chemosensing uses the benefits of statistical models, chemometric tools, and ML algorithms to not only measure pollutant concentrations but also predict their temporal variations and ecological effects. These methods enable the estimation of contaminant fluxes, transformation kinetics, bioavailability, and even potential toxicity, thereby expanding the interpretive power of GC-MS beyond static analysis [2,18,27,33].

Jirayupat et al. [48] developed NPFimg, a machine learning–based approach that integrates image processing with GC-MS data to automatically identify chemo- and biomarker features, offering a more reliable alternative to conventional peak picking. Niarchos et al. [27] introduced chemosensing as part of an early warning system that combines quantitative outputs with effect-based endpoints to signal environmental hazards in real time, before they escalate. Duff et al. [16] utilized portable GC-MS methods for rapid, on-site screening of organic pollutants in soil and water, demonstrating their applicability for field-based environmental incident monitoring.

This shift to quantitative frameworks supports a more proactive approach in environmental risk management, regulatory compliance, and ecosystem health monitoring. The integration of high-resolution data with predictive analytics enables early intervention and long-term trend forecasting, positioning GC-MS chemosensing as a cornerstone of next-generation environmental surveillance systems [16,27,33,49].

To provide context, Table 2 summarizes selected case studies where GC-MS has been applied for quantitative chemosensing in environmental applications, illustrating how advanced analytical and data-driven approaches enable robust measurement and interpretation of chemical signals.

Table 2. Selected case studies highlighting quantitative chemosensing in GC-MS environmental applications.

Application Area	Description	Ref.
Pesticides and Pharmaceuticals	Analysis of 113 pesticides in brown rice, red pepper and orange	[50]
	Analysis of 222 pesticides in seven different vegetables and fruits	[51]
	Analysis for 283 pesticides in pepper samples of Çanakkale province (Turkey)	[52]
	Analysis of 311 pesticides in Loamy sand agricultural soils	[53]
	Analysis of 19 pesticides in 30 types of cereals	[54]
	Analysis of non-steroidal anti-inflammatory drugs and estrogenic hormones in water	[55]
	Quantification of salicylic acid, acetylsalicylic acid, nalidixic acid, ibuprofen, phenacetin, naproxen, ketoprofen, meclofenamic acid and diclofenac in South African surface water	[56]
	Quantification of 41 pharmaceuticals in the geological depression of Rio Grande do Sul State, Brazil	[57]

Table 2. *Cont.*

Application Area	Description	Ref.
Microplastics and additives	Qualitative and quantitative analysis 12 of the most common plastic polymers in environmental samples	[58]
	Quantitative analysis of 12 common plastic polymers applying CaCO3 as a catalyst in pyrolytic behavior of polymers	[59]
	Quantitative analysis of plastics in samples of human tissues	[60]
	Quantification of plastic particles (diameter $\geq$ 700 nm) in human whole blood from 22 healthy volunteers	[61]
	Evaluation of Py-GC–MS for quantification of micro- and nanoplastics in human blood with a pilot study of the Australian population	[62]
Volatile organic compounds	Analysis of volatile organic compounds in eight kinds of red and green huajiao spice from different regions of China	[63]
	Identification and quantification of 104 volatile organic compounds in fermented sea bass	[64]
	Review of GC–MS analysis of volatile organic compounds in exhaled breath as biomarkers for cancer, pulmonary and infectious diseases	[65]
	Identification and quantification of 43 volatile organic compounds in raw, 65 °C- and 135 °C-treated milk	[66]
	Evaluation of a thermal desorption-gas chromatography-mass spectrometry-ion mobility spectrometry system for standardized quantification of volatile organic compounds	[67]
Industrial and agricultural pollutants (e.g., nitrophenols, pesticides)	Review of comprehensive two-dimensional gas chromatography–mass spectrometry methodologies for analysis of ultra-trace organic pollutants in environmental matrices	[68]
	Quantification of 19 organic pollutants (PAHs, BTEX, alkylphenols, tributyltin and diethylphthalate) in soils irrigated with agro-industrial wastewater	[69]
	Identification of organic pollutants in distillery wastewater and assessment of phytotoxic, cytotoxic and genotoxic effects	[70]
Early warning systems	Identification of mildew markers (1-octen-3-ol and 3-octanone) in japonica rice	[71]
	Remote sampling and identification of hazardous air pollutants using drone-mounted solid-phase microextraction coupled with portable gas chromatography–mass spectrometry	[72]
	Analysis of 16 polycyclic aromatic hydrocarbons in particulate matter ($PM_{2.5}$ and PM_{10}) from Hanoi, Vietnam using gas chromatography–tandem mass spectrometry	[73]
	Quantification of pesticide residues in honey bees, pollen, honey, vegetables and other matrices in Italy	[74]

3. Sample Preparation Trends in GC-MS-Based Chemosensing

The accuracy and sensitivity of GC-MS-based chemosensing heavily depend on the efficiency and reproducibility of the sample preparation process. The role of sample preparation as the critical initial step within the integrated GC-MS chemosensing workflow is highlighted in Figure 1. In environmental applications, complex matrices such as surface water, wastewater, sediments, and biota contain diverse organic and inorganic constituents that can interfere with the detection and interpretation of chemical signals. Therefore, robust sample preparation techniques are essential not only for isolating analytes of interest

but also for preserving the chemical information necessary for chemosensing, such as retention behavior and fragmentation patterns [15,75,76].

Traditional extraction methods. Classical techniques such as liquid–liquid extraction (LLE) and solid-phase extraction (SPE) have long been foundational in environmental sample preparation due to their operational simplicity and broad compatibility with regulatory guidelines. These methods are still widely employed in environmental monitoring programs for isolating organic pollutants, particularly when targeting hydrophobic compounds in aqueous matrices. SPE, in particular, remains a preferred method for pre-concentrating trace analytes due to its effectiveness in enriching non-polar substances [76].

However, traditional techniques also present notable limitations, including high solvent consumption, extended processing times, and relatively low selectivity, which hinder their scalability in high-throughput or real-time chemosensing workflows. As environmental monitoring shifts toward automation and miniaturization, these conventional methods are increasingly complemented or replaced by greener and faster alternatives [75,77].

Modern microextraction techniques. In response to the demand for greener and more efficient analytical workflows, advanced sample preparation strategies such as solid-phase microextraction (SPME), stir-bar sorptive extraction (SBSE), and dispersive liquid–liquid microextraction (DLLME) have gained prominence. These solvent-minimized or solvent-free techniques offer enhanced sensitivity and selectivity for volatile and semi-VOCs while minimizing environmental impact. Their miniaturized format also supports high-throughput sampling and integration with in situ or on-site monitoring platforms. For example, SPME-GC-MS enabled high-resolution temporal and spatial profiling of environmental contaminants, supporting exposomic applications and fine-scale ecological assessments [7,78,79]. Similarly, Peñalver et al. (2022) [77] applied a non-targeted DLLME–GC-MS strategy for the identification of a wide range of environmental pollutants, including chlorinated hydrocarbons, in coastal seawater. Their method achieved high sensitivity and selectivity, demonstrating the potential of DLLME–GC-MS for real-world monitoring applications. Tian et al. (2025) [78] discussed DLLME–GC-MS among other advanced microextraction methods for VOCs, highlighting its efficacy for trace-level analysis in complex matrices such as groundwater.

To illustrate these approaches more clearly, Figure 2 presents schematic workflows of three selected sample preparation techniques: SPE, DLLME, and SPME. These methods were chosen as representative examples because they cover traditional, solvent-minimized, and solvent-free strategies, respectively. The schemes highlight the main steps involved in coupling sample preparation with GC-MS chemosensing for environmental water analysis.

These techniques preserve analyte integrity, minimize matrix interference, and enable efficient chemosensing workflows, particularly relevant in regulatory monitoring and non-targeted environmental screening.

Online and automated sample preparation: The automation and online coupling of sample preparation with GC-MS systems are increasingly adopted to support real-time environmental monitoring. These platforms reduce operator variability, enhance method reproducibility, and enable rapid screening of complex matrices such as wastewater, river water, and groundwater. Recent advances demonstrate how automation and machine learning enhance the robustness and efficiency of GC-MS analysis: Ferracane et al. [80] optimized fast automated workflows for quantitative analysis of fatty acid methyl esters, Fan et al. [81] developed DeepResolution2 to fully automate untargeted GC-MS data interpretation with improved peak resolution and quantification, while Nam et al. [82] introduced scripting tools for GC×GC-MS that rapidly classify compound groups in complex mixtures. Sciex and Phenomenex presented an automated SPE system for PFAS monitoring in drinking water, enabling ppt-level detection with consistent recovery and

precision. AISTI Science implemented an online SPE-FastGC/MS/MS system to monitor pesticide residues in river water, supporting fast and automated field deployment.

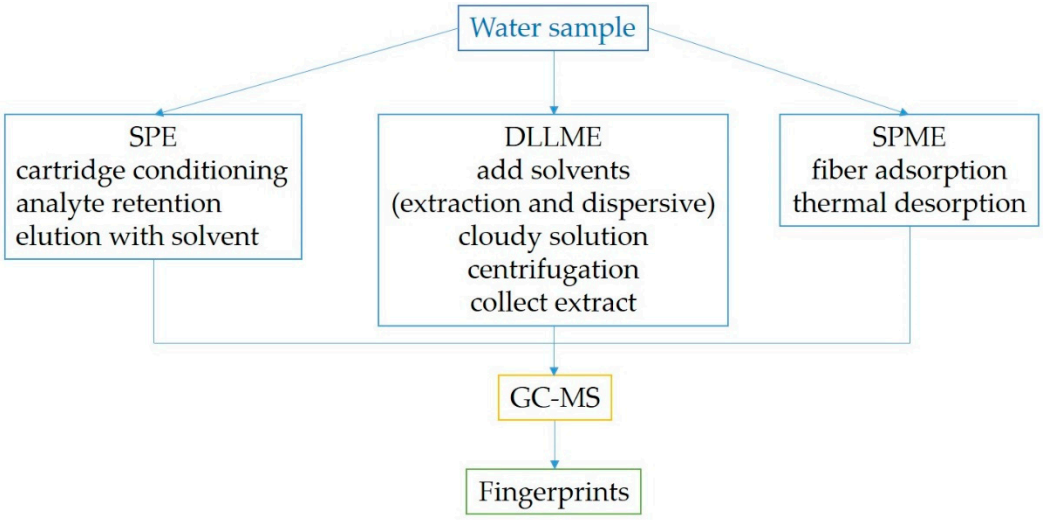

Figure 2. Schematic workflows of selected sample preparation techniques for GC-MS chemosensing of water samples.

Towards sustainable and high-throughput preparation: The ongoing direction toward greener and more efficient analytical chemistry has accelerated the development of sustainable sorbents, miniaturized extraction systems, and reusable platforms. Recent innovations include the application of nanostructured materials, bio-based polymers, and molecularly imprinted polymers (MIPs), which offer enhanced selectivity, high sorption capacity, and operational reusability, key features for sustainable GC-MS workflows in environmental analysis [75,76].

These eco-friendly strategies are particularly valuable for high-throughput screening of pollutants in complex matrices, supporting long-term monitoring with reduced environmental burden and cost. The evolution of sample preparation technologies is illustrated in Figure 3, which contrasts classical solvent-intensive techniques with modern, miniaturized, and automated methods across key analytical stages.

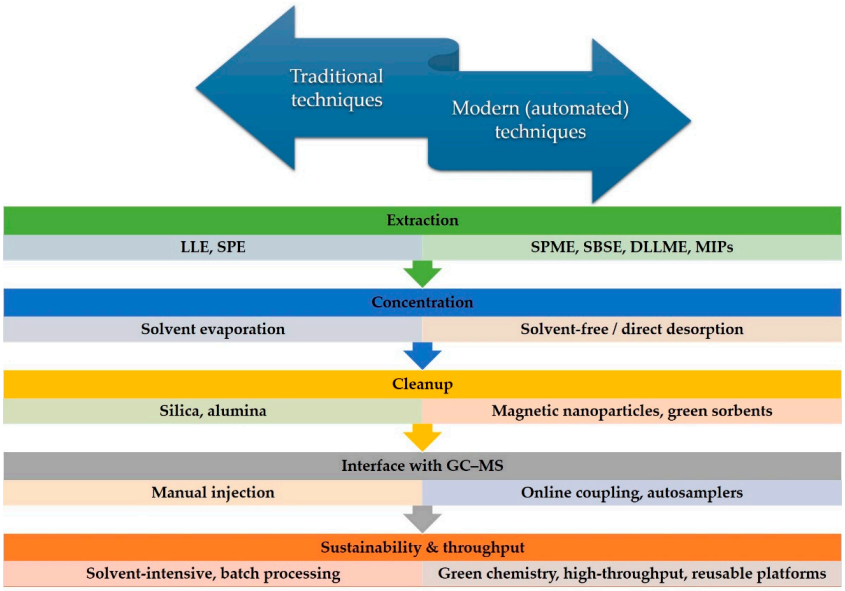

Figure 3. Evolution of sample preparation strategies in GC-MS based environmental chemosensing, highlighting the shift from traditional methods to modern, green, and automated approaches.

4. The Role of Atomistic Calculations in Complementing GC, MS, and GC-MS Analytical Methods

4.1. Introduction to Atomistic Calculations

Atomistic calculations have steadily become one of the most important components of modern research. These methods allow researchers to explore and predict the behavior of matter at an atomic level and they make it possible to simulate molecular structures, reaction pathways, energy landscapes, and dynamic processes, delivering results that complement and often guide experimental investigations. By solving the Schrödinger equation, atomistic methods offer insight at a resolution that is unavailable through macroscopic techniques alone [83–85].

In chemistry, atomistic simulations help in understanding reaction mechanisms, predicting thermodynamic and kinetic properties, designing catalysts, and modeling the electronic structure of molecules and materials [86–90]. In physics and materials science, they provide essential insights into phenomena such as phase transitions, band structure, defect formation, and surface interactions in solids, nanomaterials, and molecular crystals [91–95]. In biology and biophysics, quantum and classical atomistic approaches are widely used to study enzyme mechanisms, drug–receptor interactions, and the folding and stability of biomolecules [96–99]. The power of these calculations lies in their generality, since they allow from modeling small gas-phase molecules to simulating large solvated biomolecular complexes or condensed-phase materials.

With the increasing power of computers and the development of efficient algorithms, atomistic calculations have also become highly accessible for applied and interdisciplinary research. In environmental science, for instance, they are routinely employed to study the degradation of pollutants, sorption processes, and chemical transformations in water, air, and soil matrices [100–103]. The integration of collected data into ML workflows is further expanding their role in predictive modeling and screening studies [104,105]. Such versatility makes atomistic methods not only tools for understanding but also engines for discovery, enabling the design of new molecules, materials, and sensors before they are synthesized or fabricated.

Within the context of analytical chemistry, and particularly GC, MS, and combined GC-MS methods, atomistic calculations serve a crucial complementary function. While GC-MS provides robust experimental data on molecular identity and abundance, it often lacks direct mechanistic insight into fragmentation pathways, reactive intermediates, and the stability of detected species. Atomistic calculations help bridge this gap by allowing researchers to model the molecular structure and reactivity of analytes, simulate degradation and fragmentation mechanisms, and predict molecular properties such as ionization potential, bond dissociation energies, and electron affinity [106–108]. This mechanistic layer of interpretation is especially critical in environmental water analysis, where identifying and understanding the fate of pollutants under complex conditions is of both scientific and regulatory importance.

Atomistic methods can be broadly classified based on their underlying theoretical foundation into four main categories: wavefunction-based methods, electron density methods, semiempirical methods, and hybrid methods.

Wavefunction-based methods are the most fundamental quantum mechanical approaches, in which the electronic structure of a molecule is described explicitly through the many-electron wavefunction. The most prominent example is the Hartree–Fock (HF) method, a mean-field approximation that accounts for electron–electron repulsion in an average manner. While useful, HF neglects electron correlation, which is a critical component for achieving reasonable accuracy.

Extensions of the HF method that incorporate electron correlation are collectively known as post-HF methods. Some of the most widely used among these are Møller–Plesset perturbation theory (MP2), Coupled Cluster methods (such as CCSD and CCSD(T)), and Configuration Interaction. These methods offer high accuracy and are often used as benchmark standards; however, they are computationally expensive and typically limited to small molecular systems. Post-HF methods are particularly valuable for the detailed analysis of specific chemical processes, such as bond cleavage, radical formation, or proton-coupled electron transfer, especially in the context of pollutant degradation [109,110].

Methods based on electron density are built on the principle that all ground-state properties of a system can be determined from its electron density, rather than its many-electron wavefunction. This conceptual shift, formalized in the Hohenberg–Kohn theorems, significantly reduces computational cost while maintaining reasonable accuracy. The foundation of these methods is the density functional, which is a mathematical expression that relates the electron density to the system's total energy. While Density Functional Theory (DFT) is widely regarded for offering one of the best accuracy-to-cost ratios in atomistic modeling, it faces the challenge that no exact universal functional exists. Instead, a vast library of approximate functionals has been developed, each optimized for different classes of chemical systems or properties. Some well-known functionals are B3LYP (a hybrid functional popular for organic molecules and general chemistry applications) [111–114], PBE (widely used in solid-state and materials science) [115,116], M06 family (often applied to main-group thermochemistry and non-covalent interactions) [117–120], ωB97X-D (functional that includes long-range corrections and dispersion interactions, suitable for large and weakly interacting systems) [121,122]. By now, it has been demonstrated so many times that the choice of functional can significantly influence results. Nevertheless, its versatility and reliability make DFT a method of choice for modeling molecular structures, reaction mechanisms, thermodynamic parameters, and charge distributions.

Semiempirical quantum methods are a special class of techniques designed to reduce computational cost while preserving essential features of quantum mechanical accuracy [123]. These methods are particularly valuable when dealing with large systems or when rapid screening of numerous molecular structures is required. Semiempirical methods simplify electronic structure calculations by using empirically derived parameters, often obtained from experimental measurements or high-level theoretical data [124,125]. Like the more rigorous methods, they can be based on either wavefunction or electron density frameworks.

The best-known wavefunction-based semiempirical methods include MNDO, AM1, PM3, and PM6, foundational methods with increasing parameterization and accuracy [126–128]. PM7 method [129] is the most advanced in this family, developed by Dr. James Stewart [129]. PM7 is known for its ability to compute properties such as heats of formation with reasonable accuracy and extremely low computational demands.

In parallel, density-based semiempirical approaches have seen substantial advancements through the development of Density Functional Tight-Binding (DFTB) methods [130–133]. Among these, the GFN (Geometry, Frequency, Non-covalent) family, GFN1-xTB, GFN2-xTB, and GFN-FF, developed by Prof. Stefan Grimme and coworkers, stand out as the most powerful and broadly applicable tools in this category [123,134–137]. These methods are widely used for structure optimization, estimating thermodynamic properties, and simulating fragmentation in large or flexible molecular systems.

The computational efficiency of semiempirical methods enables their use in high-throughput screening, rapid conformational searches, and even in real-time simulations, such as those required in automated fragmentation algorithms and mass spectrum predictions.

Hybrid and multiscale methods are a special class of computational techniques that utilize the strengths of both quantum mechanical accuracy and computational efficiency. These methods divide a molecular system into distinct regions, each treated with a different level of theory depending on its relevance to the process under investigation [138,139]. The general strategy is to apply a high-level quantum mechanical method (such as DFT or even post-HF) to the chemically active region, typically where bond-breaking, electron transfer, or adsorption occurs, while using a lower-level method (such as semiempirical quantum mechanics (SQM) or even molecular mechanics (MM)) for the surrounding environment or less critical parts of the system.

For example, in the context of environmental GC-MS applications, one might consider the use of two-dimensional adsorbent surfaces such as graphene for capturing small analytes [140]. The majority of the extended adsorbent (e.g., graphene, MoS_2, or a functionalized silica surface) can be treated with a computationally inexpensive method, while the adsorption site and the interacting molecule are modeled using DFT for an accurate description of non-covalent interactions, charge transfer, or surface reactivity. The QM/SQM or QM/MM approaches offer a substantial speed-up without compromising accuracy at the chemically relevant site.

There are several relevant examples where hybrid methods have been applied in this context. In a recent study by Riyaz and Goel [141], QM/MM techniques were used to investigate the selectivity and permeability of nitrogen-passivated nanoporous graphene membranes for arsenate and chromate removal. Treating the pore region with DFT and the rest of the sheet with molecular mechanics, they showed that target molecules interact via hydrogen bonding and physisorption, with diffusion barriers indicating high selectivity for certain pore sizes. While focused on water purification, this work shows how hybrid methods can reveal analyte–surface interactions, adsorption stability, and selective diffusion in 2D materials. These insights can support the design of improved retention materials and selective coatings for GC-MS applications.

In a recent study by Mollaamin and Monajjemi (2023) [142], a sophisticated ONIOM hybrid method was applied to investigate CO_2 adsorption on transition-metal-doped graphene nanosheets with iron, nickel, and zinc as dopants. By combining DFT (CAM-B3LYP/6-31+G(d,p), LANL2DZ) with semiempirical methods and classical force fields, they captured both local adsorption chemistry and extended sheet behavior. Their results showed strong CO_2 affinity via cooperative donation–back-donation interactions, supported by favorable dipole moments and Gibbs free energies. Although aimed at gas sensing, these insights are directly transferable to GC-MS workflows, where functionalized 2D materials could serve as selective stationary phases or microextraction membranes. Hybrid methods like ONIOM can thus provide valuable mechanistic guidance for designing selective retention and separation materials in environmental GC-MS applications.

4.2. Software Packages and Codes for Performing Atomistic Calculations

The remarkable growth of computational materials science in recent years has led to the development of a broad range of software packages designed to perform atomistic simulations efficiently, many of which can now operate on standard personal computers. In general, these tools can be divided as open-source, free for academic use, or commercial. Each class offers a distinct advantage depending on user needs, project scale, and available financial and computational capabilities.

Open-source software remains a vital foundation of academic research thanks to its transparency, adaptability, and active development communities. For molecular-scale systems, PSI4 [143–145] provides high-level quantum chemistry methods, while Multiwfn [146–149] serves as a versatile platform for advanced wavefunction analysis.

The latest version of PSI4 (version 1.10) is available at the official GitHub repository https://github.com/psi4 (accessed on 1 August 2025), while Multiwfn is freely available at the official website of Prof. Tian Lu http://sobereva.com/multiwfn/ (accessed on 1 August 2025). When discussing semiempirical methods, the xTB code [123,134–137] developed by Grimme's group has gained particular popularity, as it enables rapid preoptimization, conformer searching, and molecular dynamics for systems ranging from small organic molecules to large nanoclusters using the GFN family of methods. Additionally, its GFN-FF force field further extends this capability by delivering robust atomistic simulations with wide-ranging chemical coverage. Recently, the long-awaited g-xTB method has become available to users, currently only on Linux-based platforms [150]. The software tools developed by Grimme's group are freely accessible through their official GitHub repository at https://github.com/grimme-lab (accessed on 1 August 2025), ensuring easy access for researchers worldwide.

Still in the area of semiempirical methods, MOPAC [126–129] has long been present in the field as one of the most important tools for atomistic calculations, providing robust PM-family Hamiltonians for efficient geometry optimizations, thermochemical calculations, and electronic property predictions across a broad range of molecular systems. Its continued development, led by Prof. James Stewart, has ensured compatibility with modern computational workflows while maintaining user-friendliness and fast performance, even for relatively large organic and organometallic compounds. The MOPAC software has been for a long time freely available only for academic use through its official distribution page at http://openmopac.net. However, since 2022 it has been open-source and available at the official GitHub repository https://github.com/openmopac/mopac (accessed on 1 August 2025). MOPAC is further maintained by the The Molecular Sciences Software Institute (MolSSI, https://molssi.org/, accessed on 1 August 2025).

For simulations based on force fields, LAMMPS [151,152] and GROMACS [153–160] are among the most widely adopted open-source molecular dynamics engines. LAMMPS is especially well-suited for hybrid and inorganic materials, while GROMACS, although historically tailored for biomolecules, has also seen applications in complex material and solvent systems [161].

Free-for-academic software is one more very important class, combining advanced capabilities with no-cost licenses for research. A prominent example is ORCA [138,162–169], which supports a wide spectrum of DFT and wavefunction-based methods, hybrid functionals, and TD-DFT, making it highly valuable for modeling clusters, dopants, and excited-state properties. The continuous improvements in ORCA's performance and scalability have made it a workhorse for many sophisticated electronic structure studies. Just recently, a new version of ORCA (ORCA 6.1) has been launched. Like all other revisions and ORCA tools, it is available at the official portal https://orcaforum.kofo.mpg.de/app.php/portal (accessed on 1 August 2025), after registration.

In parallel with traditional installation-based packages, cloud-based modeling platforms have gained ground thanks to their simplicity and accessibility. One noteworthy academic resource is atomistica.online (https://atomistica.online, accessed on 1 August 2025) [170–172], which provides a fully browser-based environment for semiempirical calculations, supporting engines such as xTB, MOPAC, and SHERMO [173]. The platform also includes utilities for building molecular dynamics systems, constructing ionic liquid ion pairs, performing conformer searches with RDKit [174], and generating reduced density gradient plots via Multiwfn. These features are seamlessly integrated in an easy-to-use web interface, eliminating the need for complex local setups. Recent additions include models such as OMol25 and UMA, broadening its applicability in modern molecular screening workflows.

Commercial software solutions, in turn, target both industrial and high-end academic users with powerful, fully supported packages, often featuring intuitive GUIs and tightly integrated toolchains. Notable options include the Materials Science Suite from Schrödinger (https://www.schrodinger.com, accessed on 1 August 2025), ADF from SCM (https://www.scm.com, accessed on 1 August 2025), and QuantumATK by Synopsys (https://www.synopsys.com/manufacturing/quantumatk.html, accessed on 1 August 2025). These platforms combine periodic and molecular DFT capabilities with advanced MD engines, postprocessing tools, and ML-ready descriptor generators. Schrödinger's suite, for example, integrates Quantum ESPRESSO for DFT and Desmond for MD in a user-friendly workflow, while ADF offers periodic DFT through its BAND module. QuantumATK similarly supports robust atomistic modeling pipelines, including band structure analysis and property prediction. On the commercial side of online platforms, Rowan (https://rowansci.com, accessed on 1 August 2025) and Samson (https://www.samson-connect.net, accessed on 1 August 2025) represent modern examples of browser-based interfaces with professional support.

In practice, each of these categories provides complementary benefits. Open-source software offers maximum transparency and collaborative potential, while free-for-academic licenses lower barriers to advanced methods. Commercial platforms, though requiring investment, deliver premium features and expert assistance. Depending on the goals of a study, researchers can select and combine these tools for effective and reliable atomistic modeling workflows.

4.3. Atomistic Calculations as a Complement to GC, MS, and GC-MS

Atomistic calculations play a crucial complementary role, enabling researchers to model and predict processes that are difficult or impossible to probe experimentally. This section highlights several major ways in which atomistic methods enhance analytical interpretations: modeling fragmentation, mapping molecular reactivity, and exploring pollutant behavior in dynamic aqueous environments.

4.3.1. Supporting Interpretation of Fragmentation and Degradation

Mass spectrometry is a powerful tool for identifying chemical species based on their m/z ratios. However, for complex or novel analytes, fragmentation pathways are not always straightforward, and experimental spectra can be difficult to interpret without mechanistic insight. Atomistic calculations, particularly those based on DFT and semiempirical methods, can help in this area, by enabling the prediction of fragmentation mechanisms and the identification of likely intermediates.

One of the most essential fundamental applications of DFT in this context is the calculation of bond dissociation energies (BDEs), which provides direct information about the relative stability of chemical bonds. By identifying the weakest bonds in a molecule, one can anticipate which fragments are most likely to appear in the mass spectrum after ionization. This approach is beneficial for understanding EI and CID processes.

Lienard et al. (2015) [175] applied DFT calculations to predict the autoxidation sensitivity of active pharmaceutical ingredients by estimating C-H bond dissociation energies across a diverse set of 45 compounds. Comparing different DFT functionals, they identified PBE as a good balance between speed and accuracy for routine stability risk assessment. Although aimed at formulation stability, this BDE-based approach is directly valuable for GC-MS structural analysis by highlighting labile bonds, aiding the interpretation of fragmentation pathways, and predicting likely degradation products.

Andersson et al. (2017) [176] developed an automated DFT-based protocol to estimate C-H BDEs and predict autoxidation sensitivity in drug candidates. Their results showed

that multiple functional groups usually stabilize radicals involved in degradation, and their workflow makes such calculations accessible even to non-specialists. This protocol is valuable because it enables scientists to combine BDE concepts with experimental data, directly supporting GC-MS structural analysis by identifying labile bonds and potential degradation fragments early in the development process.

The protocols developed in the previously mentioned studies [175,176] motivated our research group to adopt a similar approach, particularly focusing on hydrogen bond dissociation energies (H-BDE) to identify molecular sites where degradation could be initiated [177,178]. In most of our studies, we employed the B3LYP density functional together with the 6-311G(d,p) basis set, providing a reliable compromise between computational efficiency and predictive accuracy.

However, instead of relying solely on physically grounded atomistic calculations, it is possible to cover a much broader chemical space by combining these methods with ML. For example, in a recent study by Shree Sowndarya et al. (2023) [179], a graph-based ML model was trained on over 530,000 DFT-calculated bond dissociation enthalpies to predict homolytic BDEs of halogenated and environmentally relevant compounds with high accuracy. Although aimed at broad chemical coverage, this work is highly relevant to GC-MS, where bond dissociation energetics define fragmentation pathways. Such predictive models can support GC-MS analysis of complex or emerging pollutants by highlighting labile bonds and improving structural assignments.

In the context of environmental water analysis, where degradation products of pesticides, pharmaceuticals, and industrial chemicals often appear in trace amounts, computational prediction of reactive intermediates and radical pathways is critical [180,181]. Atomistic methods allow for the exploration of hydrogen abstraction, hydroxylation, and oxidative cleavage, reactions frequently triggered by exposure to UV light, ozone, or advanced oxidation processes [182–184].

In addition to modeling primary fragmentation, atomistic calculations can be used to simulate the energetics and structures of degradation products, providing theoretical spectra for comparison with experimental data [185,186]. This is especially valuable in situations where tandem MS (MS/MS) is unavailable or prohibitively expensive, and researchers must rely on single-stage mass spectra and chromatographic retention times to identify unknowns. Furthermore, combining fragmentation energetics with transition state (TS) searches or intrinsic reaction coordinate (IRC) calculations allows for the mapping of complete degradation pathways, offering insight into both kinetics and thermodynamics of pollutant transformation [187,188]. These mechanistic insights can then inform environmental risk assessments and guide the development of remediation strategies.

4.3.2. Local and Global Reactivity Descriptors

Atomistic calculations, especially those based on the DFT approach, offer an array of descriptors that quantify molecular reactivity at both the local (site-specific) and global (molecule-wide) level [189,190]. These descriptors are especially valuable in environmental water analysis for understanding pollutant behavior, predicting degradation hotspots, and guiding sensor design [191,192].

Several quantum-molecular descriptors can map regions of high or low reactivity on a molecular surface. These include molecular electrostatic potential (MEP), average local ionization energy (ALIE) and topology of frontier orbitals (HOMO-LUMO topology).

MEP descriptor provides information about the distribution of electrostatic potential around a molecule. Regions of negative potential (electron-rich) are prone to electrophilic attack, while areas of positive potential (electron-deficient) are prone to nucleophilic attack [193–199]. This descriptor is particularly useful for predicting sites of oxidation

or interactions with charged species in water. The ALIE descriptor gives information about the energy required to remove an electron from a specific region on a surface of a molecule [200–204]. This descriptor may be useful for identifying regions potentially more sensitive to electron loss and oxidative degradation. ALIE could be particularly relevant for exploring the behavior of pollutants under photooxidative conditions or advanced oxidation processes.

It is essential to mention that both MEP and ALIE descriptors can be presented visually in the form of surfaces by mapping their values to the electron density surface. In this way, scientists obtain a very intuitive and describable tool to identify the most reactive molecular sites, which is essential for a deeper understanding of the results obtained by GC, MS and GC-MS experimental methods.

Topology of frontier molecular orbitals is another important concept for visually identifying the most reactive molecular sites. The spatial distribution of the highest occupied molecular orbital (HOMO) and the lowest unoccupied molecular orbital (LUMO) provides information on donor and acceptor sites [205–208]. HOMO-localized regions may be vulnerable to electrophilic attack or ionization, while LUMO-localized areas may serve as nucleophilic targets or sites for reduction.

These local descriptors allow researchers to rationalize fragmentation patterns in MS spectra, model interactions with sensor surfaces (e.g., adsorption in GC columns), and predict reactive sites in degradation processes.

In addition to site-specific information, atomistic calculations offer global descriptors that summarize the overall chemical reactivity and stability of a molecule [209–213]:

- Ionization potential (IP) and electron affinity (EA): These fundamental quantities reflect a molecule's tendency to lose or gain electrons and can be directly linked to oxidation or reduction potential in environmental reactions.
- Chemical hardness and softness: Hard molecules are generally less reactive, while soft molecules are more prone to undergo chemical transformations. These indices are derived from frontier orbital energies and provide a theoretical basis for pollutant persistence.
- Electrophilicity index (ω): This parameter quantifies a molecule's overall tendency to accept electrons and engage in reactions with nucleophiles. Molecules with high ω may react rapidly with biological nucleophiles or natural reductants in aquatic systems.
- Chemical potential (μ): Indicates the escaping tendency of electrons from a molecule, closely related to molecular stability and charge transfer behavior.

Collectively, these descriptors can be computed with relatively modest computational resources and integrated into predictive workflows. For example, they can be used to prioritize pollutants for monitoring based on reactivity, to correlate GC retention times with molecular polarity or size, or to anticipate the fate of contaminants under various oxidative treatments.

There is a vast number of published studies where global and local reactivity descriptors have been utilized to identify the reactive molecular sites, and therefore molecular sites sensitive to various types of chemical attacks that could initiate the fragmentation of molecules, while these information is very important for the understanding of the obtained experimental results via GC MS methods.

For example, in a study by Wang et al. (2014) [214], DFT and TDDFT calculations were performed to explore the photodechlorination mechanisms of 35 polychlorinated biphenyl (PCB) congeners, using BDEs and activation energies for C–Cl bond cleavage as key indicators. Their results linked the degree of ortho-chlorine substitution to ring deformation in the excited state, affecting photoreactivity and preferred dechlorination pathways. These findings directly support GC-MS studies by identifying the weakest C-Cl

bonds most prone to fragmentation, aiding structural elucidation and understanding of PCB transformation products in environmental monitoring.

In one of our studies [215], DFT calculations were used to characterize the degradation pathways of loratadine (LOR), a widely used antihistamine frequently detected in wastewater. We calculated H-BDE, identifying likely sites for oxidative and hydrolytic degradation. Local reactivity descriptors, including MEP, ALIE, and Fukui functions, highlighted the pyridine nitrogen and certain oxygen atoms as key reactive centers. These results are directly relevant for GC-MS workflows, where understanding bond strengths and reactivity patterns helps interpret fragmentation pathways and trace environmental transformation products of pharmaceutical pollutants.

4.3.3. Molecular Dynamics for Environmental Behavior

While quantum chemical methods provide valuable insights into electronic structure and molecular reactivity, they are inherently "static", i.e., they are describing molecules as fixed geometries located on a potential energy surface. However, many processes in environmental systems are dynamic in nature: molecules interact with solvents, aggregate, diffuse, and undergo conformational changes over time. To model such time-dependent behavior, molecular dynamics (MD) simulations are indispensable.

MD is a computational technique that simulates the physical movements of atoms and molecules over time by numerically solving Newton's equations of motion. Each atom is treated as a classical particle, and its trajectory is computed based on the forces acting on it. These forces are derived from the system's potential energy, which is typically described by a force field. A force field is a mathematical model that estimates the potential energy of a molecular system as a function of atomic positions. It includes terms for bond stretching, angle bending, torsional rotations, and non-bonded interactions such as van der Waals forces and electrostatics. Common empirical force fields used in MD include AMBER [216], CHARMM [217–219], and OPLS [220–225], which have been extensively parameterized for biomolecules, organic compounds, and polymers.

While classical force fields offer excellent speed and scalability, it is also possible to compute the total energy during MD simulations using quantum mechanical methods. Approaches such as Car–Parrinello MD or Born–Oppenheimer MD enable a quantum treatment of electrons, typically employing DFT. However, these methods are computationally demanding and generally restricted to small systems and short timescales. For larger systems or longer simulations, semiempirical quantum methods, such as GFN-xTB, offer a compromise between accuracy and efficiency. In fact, the recently developed force field based on the GFN-xTB approach, the GFN-FF [137], might be a game-changer in times to come, as it offers simple usage with huge coverage of elements (up to Z = 86). Just recently, Grimme's research group released the latest semiempirical method denoted as g-xTB [150], with significantly improved accuracy compared to GFN2-xTB.

In the context of environmental water analysis, MD simulations provide critical insights that complement and extend findings from GC-MS measurements. They enable researchers to explore solubility, aggregation tendencies, diffusion behavior, and interactions with sensor materials under realistic, thermally fluctuating conditions.

In our own work, we applied MD simulations together with DFT calculations to study loratadine, a widely used antihistamine frequently detected in water [215]. Through MD simulations with explicit water models, we identified key molecular regions with the strongest interactions with solvent molecules by analyzing radial distribution functions (RDFs). These interactions, especially around the chlorine atom and selected carbon atoms, highlighted sites potentially prone to hydrolysis or further degradation. When combined with our BDE calculations that indicated oxidation-sensitive sites, these MD

results provided a more comprehensive picture of loratadine's behavior under realistic aqueous conditions. This atomistic-level understanding supports the interpretation of GC-MS fragmentation patterns of loratadine and its transformation products, ultimately improving confidence in compound identification and environmental risk assessments.

In a recent study, Dixon et al. (2022) [226] combined advanced MD simulations with hydrogen-deuterium exchange mass spectrometry (HDX-MS) to solve the structural and dynamic determinants of targeted protein degradation. Their enhanced MD simulations, guided by HDX-MS data, revealed key conformational ensembles of E3 ligase complexes, while proteomics experiments confirmed predicted ubiquitination sites. This integrative approach highlights how atomistic modeling and mass spectrometry can synergistically explain and predict protein modification pathways, setting a benchmark for linking simulations with MS data in complex biological and analytical systems.

4.3.4. Searching Conformational Space

Gaining insight into the conformational preferences of organic compounds is essential for understanding their behavior in GC-MS and related analytical techniques. Many molecules contain flexible side chains, heterocyclic systems, and multiple functional groups that often allow these molecules to adopt various spatial arrangements, which shift depending on temperature, solvent conditions, or sample matrix effects. These different conformers can vary in stability, steric hindrance, and hydrogen-bonding patterns, which in turn may alter fragmentation routes, affect retention characteristics, and influence ionization efficiency, all factors that shape the observed mass spectra.

Atomistic calculations that aim to model bond dissociation energies, reactivity descriptors, or local reactive sites must account for this structural flexibility to provide reliable predictions. Relying on a single, arbitrarily chosen geometry risks overlooking low-energy conformers or reactive motifs that could dominate the experimental signal. Therefore, systematic conformational sampling is a critical prerequisite for trustworthy computational support of GC-MS analysis. Exploring the accessible conformational space allows researchers to identify representative structures, determine the ensemble-averaged properties, and connect experimental observations to fundamental molecular behavior with greater confidence.

GOAT implementation in ORCA. A key challenge in conformational analysis is to move beyond finding a single optimized geometry and instead systematically explore the entire conformational ensemble relevant to experimental conditions. In this context, ORCA's Global Optimizer Algorithm (GOAT) offers a robust framework. GOAT combines principles of basin-hopping, minima-hopping, simulated annealing, and taboo search to locate the global minimum on a potential energy surface efficiently (PES) and identify nearby low-energy conformers [227–229].

The algorithm works by first optimizing the initial input structure to the nearest local minimum and then performing uphill moves in random directions to escape local minima, followed by new optimizations. By repeating this cycle, GOAT samples diverse regions of the PES, gathering a conformational ensemble that is relevant for thermodynamic and spectroscopic averaging. Unlike standard local optimizations, this approach systematically collects structures, providing insight into conformer energies, degeneracies, and entropic contributions.

GOAT is highly parallelizable, allowing multiple "workers" to independently sample and optimize candidate structures, making it suitable even for moderately large systems. While it can be used with DFT, it is typically paired with faster semi-empirical methods, such as GFN2-xTB, to manage computational costs. Ultimately, GOAT enables researchers to generate a well-characterized ensemble of conformers, facilitating more

robust predictions of reactivity, fragmentation, and spectral behavior relevant to GC-MS and environmental analysis.

The GOAT procedure has been particularly useful for our research group recently, as we used it to find global minima of hundreds of ionic liquids we studied for building ML models to predict density and viscosity [170]. Specifically, we applied the GFN-FF force field during the GOAT global minimum search.

CREST method and code: The Conformer–Rotamer Ensemble Sampling Tool (CREST) is a powerful utility built around the GFN-xTB family of semi-empirical methods, developed to systematically explore and sample the low-energy chemical space of molecular systems [230–236]. Its primary goal is to generate a diverse and thermodynamically relevant ensemble of conformers and rotamers, which are essential for understanding molecular properties under realistic conditions. CREST handles not only conformers but also rotamers to account for the complete accessible conformational ensemble.

The core CREST workflow, called iMTD-GC (iterative metadynamics and genetic crossing) [236], combines metadynamics sampling with a genetic crossing strategy. In this procedure, bias potentials are applied to encourage the molecule to escape already-visited minima, while the genetic crossing step creates new structures by recombining internal coordinates from existing low-energy structures. These candidate geometries are then optimized and filtered. This approach ensures efficient sampling of relevant conformers while systematically avoiding duplication, leading to a representative ensemble of low-energy structures.

Beyond standard conformer searches, CREST offers workflows for explicit solvation (via Quantum Cluster Growth, QCG), constrained sampling, protonation/deprotonation site screening, and even automated fragmentation product searches relevant to mass spectrometry (MSREACT). The built-in capabilities for calculating ensemble entropies and free energies also make the software valuable for thermochemical and spectroscopic studies.

For demonstration purposes, we describe our application of the CREST and GOAT workflows, employing the GFN2-xTB method to identify the lowest-energy conformer of ibuprofen, a widely studied pharmaceutical compound and recognized water pollutant due to its extensive use in the pharmaceutical industry. The initial structure of ibuprofen was intentionally distorted, with its isobutyl group arranged in an almost linear conformation, to challenge the CREST and GOAT algorithms and observe the resulting optimized structures. The starting geometry and the resulting global minimum structures are shown in Figure 4.

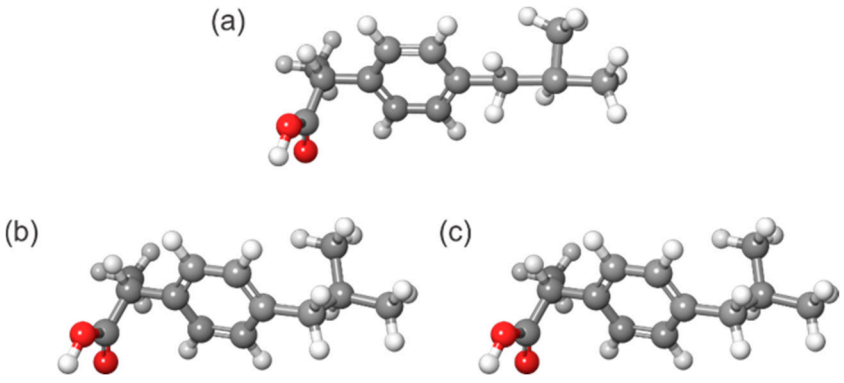

Figure 4. (**a**) starting deformed structure of ibuprofen, and lowest-energy conformation of ibuprofen obtained by (**b**) CREST and (**c**) GOAT workflows, using the GFN2-xTB level of theory.

In this case, we intentionally distorted the starting geometry of ibuprofen by setting its isobutyl side chain into an unrealistic, nearly linear configuration. This provided a challenging test case for the CREST and GOAT workflows to determine whether they

could reliably recover the true lowest-energy conformation. Both workflows, applying the GFN2-xTB method, successfully optimized the molecule to essentially identical final structures, as confirmed by visual inspection of Figure 3.

To quantitatively verify this, a superposition of the two optimized geometries was performed. The superposition resulted in an RMSD value of 0.001 Å, demonstrating excellent agreement. This result illustrates the consistency of both CREST and GOAT in exploring the conformational space and locating the global minimum, even from significantly perturbed starting geometries. Of course, the best practice is to first pre-optimize the structure, for example, by using GFN2-xTB, before applying workflows to identify the global minimum conformation.

4.4. Simulation of MS Spectra Using QCxMS Codes

As already adopted, mass spectrometry plays a central role in the identification and quantification of environmental pollutants, particularly in the context of GC-MS workflows. However, interpreting complex fragmentation patterns, especially for novel or unknown compounds, can be challenging. This is where quantum chemical simulations of MS spectra offer substantial added value. The Quantum Chemical Mass Spectrometry (QCxMS) approach, developed by the Grimme's group [237–248], provides a powerful and fully automated framework for simulating EI and CID spectra using atomistic methods.

Accurate interpretation of mass spectra, particularly for environmental pollutants, their degradation products, and structurally complex molecules, often demands more than database matching or heuristic rules. The QCxMS and its successor, QCxMS2, are open-source, quantum chemistry-based programs that simulate mass spectra by modeling molecular fragmentation processes from first principles. They enable researchers to predict fragmentation patterns, explore reaction mechanisms, and generate theoretical MS spectra to aid in compound identification and structural elucidation.

QCxMS and QCxMS2. The original QCxMS program is built on Born–Oppenheimer MD (BOMD), where fragmentation is simulated by running high-energy MD trajectories of a charged molecule. Fragment ions are identified from these trajectories and used to construct the simulated spectrum. While this method is powerful and physically grounded, it can be computationally intensive, particularly for large molecules or when extensive statistical sampling is required.

The recently developed QCxMS2 represents a conceptual evolution of the method. Instead of using MD, QCxMS2 uses automated reaction network discovery to map out possible fragmentation pathways more efficiently [249]. This enables faster and more chemically intuitive identification of plausible fragments, thereby improving accessibility and scalability.

Both tools are freely available and form part of the xtb software ecosystem, which is built around the semi-empirical GFN-xTB family of methods for efficient and accurate quantum chemical calculations.

Both QCxMS and QCxMS2 aim to simulate three major MS fragmentation modes:

- EI: This mode is fully supported in both versions. It simulates ionization via an energetic (typically 70 eV) electron beam that produces an open-shell radical cation. The excess internal energy from ionization induces fragmentation and rearrangement events. QCxMS handles this through MD, while QCxMS2 employs a network-based approach to simulate possible reaction pathways following ionization.
- Dissociative Electron Attachment (DEA): In the DEA approach, a radical anion is generated. While this mode is technically supported in both QCxMS and QCxMS2, it requires DFT calculations and diffuse basis sets, significantly increasing computational

resources necessary for calculations. Furthermore, the DEA in QCxMS2 remains experimental, and users are advised to proceed cautiously when applying it.

- CID: CID is widely used to fragment (de)protonated ions produced by electrospray ionization (ESI), offering a softer alternative to EI or DEA. Although QCxMS2 does not yet provide a dedicated CID mode, its EI mode can be tuned to approximate CID spectra by lowering internal energy distributions. However, these adjustments should be benchmarked against experiments, and for more robust CID predictions, the original QCxMS is currently recommended.

One of the key strengths of both QCxMS and QCxMS2 is their seamless integration with major quantum chemistry engines, most notably xtb and ORCA. This allows users to perform fragmentation and spectrum simulations using either efficient semiempirical methods or more accurate, higher-order quantum mechanical approaches.

The xtb backend, particularly the GFN2-xTB method, offers an excellent balance between computational speed and chemical accuracy. It is particularly well-suited for medium and large molecules, which enables the simulation of hundreds of fragmentation trajectories within a feasible time frame. The method collects essential electronic and structural features of the molecular ion, making it highly effective for generating realistic mass spectra with reasonable computational demands.

For cases requiring higher accuracy, both QCxMS and QCxMS2 can interface with ORCA, DFT or composite method calculations for ionization, fragmentation, and determination of electronic structure. Although DFT provides higher accuracy, it is essential for species with complex electronic structures or in DEA simulations. However, its computational cost is significantly higher, limiting its applicability to smaller systems or benchmarking purposes.

This dual compatibility offers users a flexible platform: for routine environmental pollutant screening, GFN2-xTB provides reliable and rapid results; for detailed mechanistic studies or high-accuracy validation, DFT-level simulations can be selectively employed. In the forthcoming examples, the effectiveness of GFN2-based QCxMS workflows will be demonstrated in practical environmental contexts, showing how fast, first-principles-based MS simulations can complement and enhance GC-MS analyses.

Input files for QCxMS workflows can be conveniently prepared using atomistica.online molecular modeling platform (freely available for academic purposes at https://atomistica.online, accessed on 1 August 2025), which provides a dedicated web-based tool for generating the required input parameters.

For demonstration purposes, we applied the EI method of QCxMS2 to simulate the mass spectrum of 2-hexanone, an industrially relevant pollutant similar to 2-pentanone and representative of mid-sized ketones. Using the automated workflow of QCxMS2, we obtained results (Figure 5) that qualitatively agree very well with the experimental results available at the NIST database (https://webbook.nist.gov/cgi/cbook.cgi?ID=C591786&Mask=200#Mass-Spec, accessed on 1 August 2025).

While differences in relative intensities are present, the simulated mass spectrum of 2-hexanone obtained with QCxMS2 shows excellent qualitative agreement with the reference NIST spectrum. Both spectra feature a dominant peak at m/z 43, characteristic of ketone fragmentation, as well as a prominent peak at m/z 58, which is similarly well reproduced. The overall fragmentation pattern in the lower m/z region (20–60), including peaks around 29 and 41, is also consistent between simulation and experiment. Together, the ability of QCxMS2 to accurately reproduce key fragment ions and their relative abundances highlights its value in complementing GC-MS analyses and supports its use in environmental pollutant identification.

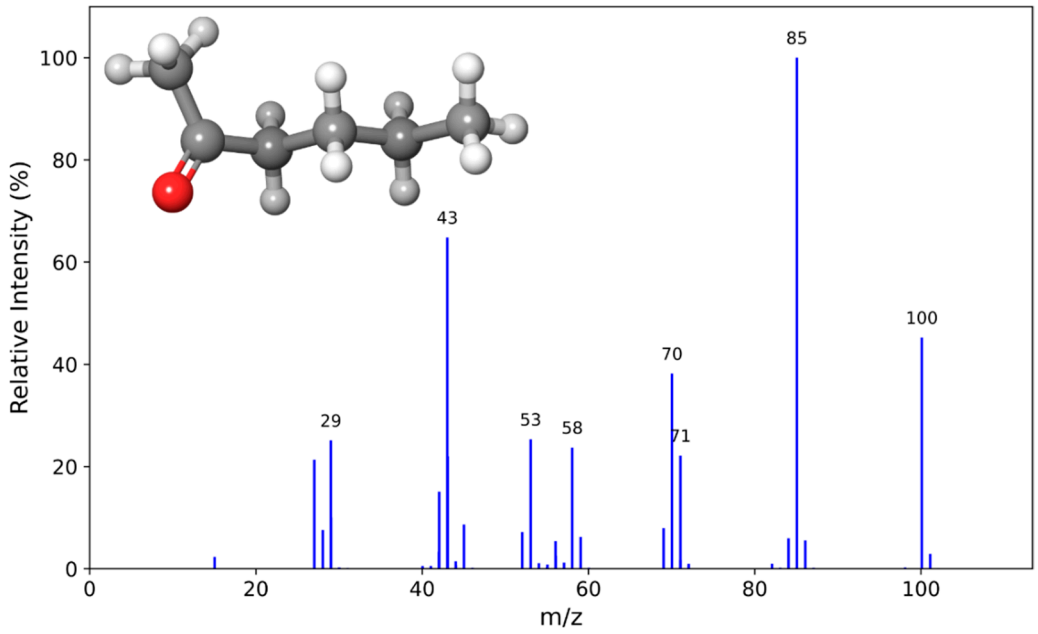

Figure 5. Simulated MS spectrum of 2-hexanone using the QCxMS2 code at GFN2-xTB level of theory (inset: molecular geometry of 2-hexanone).

To provide a concise overview of the principal atomistic approaches discussed in this section, we have summarized the key features, outputs, and relevance in Table 3. This table highlights how atomistic calculations can be applied to complement GC-MS workflows.

Table 3. Summary of principal atomistic approaches that complement GC-MS workflows in environmental analysis.

Category	Principle and Typical Use	How It Complements GC–MS	Key Output	Ref.
Methods QM calculations: ab initio, DFT, semiempirical, hybrid MD simulations: Force field or ab initio	QM: DFT for accuracy-cost balance; semiempirical (PM7, GFN2-xTB, GFN-FF) for speed; hybrid QM/MM for local accuracy in large systems, post-HF for benchmarks MD: Classical: (AMBER/CHARMM/OPLS), Semiempirical: (GFN-xTB/FF), Ab initio (density functional)	QM: Mechanistic insights into fragmentation, stability, and transformation pathways MD: Model solvation, diffusion, aggregation, and stability relevant to aqueous analysis	QM: BDEs, activation barriers, reaction thermodynamics MD: RDFs, solvation shells, diffusion coefficients, conformational dynamics	[134,136,138,167]
Descriptors (local/global reactivity)	Local (MEP, ALIE, HOMO/LUMO topology) and global (IP, EA, hardness/softness, electrophilicity) indices from electronic structure	Pinpoint reactive sites, degradation hotspots, and fragmentation-prone bonds; prioritize pollutants	Mapped surfaces and scalar indices linked to fragmentation/persistence	[198,202]
Conformational search space (CREST, GOAT)	Systematic exploration of low-energy conformers/rotamers using GFN-xTB/GFN-FF; ensemble-aware modeling	Ensures reliable reactivity/BDE predictions; explains variability in retention and fragmentation	Conformer ensembles; global minima; ensemble-averaged properties	[229,232,234]
Engines/Modeling codes	ORCA (DFT/post-HF), xTB (GFN family), MOPAC (PM methods), PSI4, Multiwfn; MD engines (GROMACS, LAMMPS); QCxMS/QCxMS2 for MS simulation	Backends for structure, reactivity, dynamics, and spectrum simulation	Optimized structures, reactivity maps, simulated spectra, MD trajectories	[134,136,138,167]
Simulation of MS spectra (QCxMS/QCxMS2)	Automated EI/CID/DEA fragmentation modeling (xtb/ORCA backends); MD- or network-based	Predicts fragmentation routes and theoretical spectra; valdates/augments experimental assignments	Simulated spectra; mechanistic pathways and fragment identities	[240,245,248,249]
Online tools	atomistica.online integrating xTB, MOPAC, SHERMO, Multiwfn, browser-based workflows	Low-barrier access to semiempirical calculations, conformer search, RDG plots, and QCxMS input prep	Web workflows; inputs/outputs ready for GC-MS support	[170–179]

5. Conclusions

GC-MS continues to serve as the gold standard for analyzing complex water matrices, delivering exceptional sensitivity, selectivity, and robustness. This review has demonstrated how recent innovations, including high-resolution instruments, multidimensional separations, and portable systems, have extended GC-MS from conventional targeted detection toward a more comprehensive chemosensing platform capable of providing molecular fingerprints of environmental water samples. The combination of GC-MS with advanced data processing techniques, such as ML and chemometrics, further enables intelligent diagnostics and predictive monitoring of emerging contaminants.

A key novel perspective presented in this review is the integration of atomistic modeling alongside GC-MS workflows, including quantum mechanical and semiempirical calculations, and molecular dynamics simulations.

Nevertheless, several challenges remain to be solved. These include the need for standardized workflows and reference databases to ensure reproducibility, the complexity of handling increasingly large GC-MS datasets, the computational cost of accurate atomistic simulations, and the limited integration of experimental GC-MS data with theoretical modeling in routine practice. A solution to these challenges will be essential for transforming current innovations into widely applicable tools for environmental monitoring.

Looking ahead, future progress will depend on advances in automation, AI-driven data interpretation, and the expansion of open-access spectral databases. Furthermore, the integration of GC-MS chemosensing with complementary omics approaches offers the potential for more holistic assessments of environmental exposures. These perspectives highlight the capacity of GC-MS to evolve into a more standardized and comprehensive platform for environmental monitoring and protection.

Author Contributions: Conceptualization, S.J.A. and S.A.; Data curation, S.J.A. and S.A.; Funding acquisition, S.J.A. and S.A.; Investigation, S.J.A. and S.A.; Methodology, S.J.A. and S.A.; Project administration, S.J.A. and S.A.; Resources, S.J.A. and S.A.; Software, S.J.A. and S.A.; Visualization, S.J.A. and S.A.; Writing—original draft, S.J.A. and S.A. All authors have read and agreed to the published version of the manuscript.

Funding: The authors gratefully acknowledge the financial support of the Ministry of Science, Technological Development and Innovation of the Republic of Serbia (Grants No. 451-03-137/2025-03/200125 and 451-03-136/2025-03/200125).

Institutional Review Board Statement: Not applicable.

Informed Consent Statement: Not applicable.

Data Availability Statement: The original contributions presented in the study are included in the article material, further inquiries can be directed to the corresponding author.

Acknowledgments: The Association for the International Development of Academic and Scientific Collaboration (https://aidasco.org/ accessed on 1 August 2025.), Centrohem d.o.o. (https://www.centrohem.co.rs/ accessed on 1 August 2025.), and Serbian Natural History Society (https://spd.rs/ accessed on 1 August 2025.) who supported the research by providing part of the computer resources.

Conflicts of Interest: The authors declare no conflict of interest.

Abbreviation

Abbreviation	Meaning
ECs	Emerging contaminants
MS	Mass Spectrometry
GC-MS	Gas Chromatography–Mass Spectrometry
VOCs	Volatile Organic Compounds

AI	Artificial Intelligence
POPs	Persistent Organic Pollutants
CECs	Contaminants of Emerging Concern
TIC	Total Ion Chromatogram
TIMS	Trapped Ion Mobility Spectrometry
ML	Machine Learning
HR–ToFMS	High-Resolution Time-of-Flight Mass Spectrometry
GC×GC	Two-Dimensional Gas Chromatography
EI	Electron Ionization
CI	Chemical Ionization
NTS	Non-Target Screening
PCA	Principal Component Analysis
PLS-DA	Partial Least Squares–Discriminant Analysis
HCA	Hierarchical Cluster Analysis
SVM	Support Vector Machine
RF	Random Forest
LLE	Liquid–Liquid Extraction
SPE	Solid Phase Extraction
SPME	Solid Phase Microextraction
SBSE	Stir Bar Sorptive Extraction
DLLME	Dispersive Liquid–Liquid Microextraction
MIPs	Molecularly Imprinted Polymers
SPME-GC	Solid Phase Microextraction coupled with Gas Chromatography
PFAS	Per- and Polyfluoroalkyl Substances
AISTI	All Ion Switching Tandem Ionization
HF	Hartree–Fock
CCSD	Coupled Cluster with Single and Double excitations
DFT	Density Functional Theory
PBE	Perdew–Burke–Ernzerhof (functional)
MNDO	Modified Neglect of Diatomic Overlap
AM1	Austin Model 1 (semiempirical method)
PM3 and PM6	Parametric Method 3 and 6 (semiempirical methods)
DFTB	Density Functional Tight Binding
GFN	Geometry, Frequency, Noncovalent
GFN2-xTB	Geometry, Frequency, Noncovalent extended Tight Binding
GFN-FF	Geometry, Frequency, Noncovalent–Force Field
SQM	Semiempirical Quantum Mechanics
MM	Molecular Mechanics
QM	Quantum Mechanics
ONIOM	Our Own N-layered Integrated molecular Orbital and molecular Mechanics
CAM	Coulomb-Attenuating Method
B3LYP/6-31+G(d,p)	Becke, 3-parameter, Lee–Yang–Parr functional with 6-31+G(d,p) basis set
LANL2DZ	Los Alamos National Laboratory 2 Double-Zeta basis set
BDEs	Bond Dissociation Energies
H-BDE	Hydrogen Bond Dissociation Energies
MEP	Molecular Electrostatic Potential
ALIE	Average Local Ionization Energy
HOMO-LUMO	Highest Occupied Molecular Orbital-Lowest Unoccupied Molecular Orbital
IP	Ionization Potential
EA	Electron Affinity
MD	Molecular Dynamics
HDX-MS	Hydrogen–Deuterium Exchange Mass Spectrometry
QCG	Quantum Cluster Growth
MSREACT	Mass Spectrometry Reaction (simulation tool)

QCxMS	Quantum Chemical Mass Spectrometry
BOMD	Born–Oppenheimer MD
DEA	Dissociative Electron Attachment

References

1. Vosough, M.; Schmidt, T.C.; Renner, G. Non-Target Screening in Water Analysis: Recent Trends of Data Evaluation, Quality Assurance, and Their Future Perspectives. *Anal. Bioanal. Chem.* **2024**, *416*, 2125–2136. [CrossRef]
2. Houhou, R.; Bocklitz, T. Trends in Artificial Intelligence, Machine Learning, and Chemometrics Applied to Chemical Data. *Anal. Sci. Adv.* **2021**, *2*, 128–141. [CrossRef]
3. Ganaie, M.I.; Jan, I.; Mayer, A.N.; Dar, A.A.; Mayer, I.A.; Ahmed, P.; Sofi, J.A. Health Risk Assessment of Pesticide Residues in Drinking Water of Upper Jhelum Region in Kashmir Valley-India by GC-MS/MS. *Int. J. Anal. Chem.* **2023**, *2023*, 6802782. [CrossRef]
4. Moufid, M.; Hofmann, M.; El Bari, N.; Tiebe, C.; Bartholmai, M.; Bouchikhi, B. Wastewater Monitoring by Means of E-Nose, VE-Tongue, TD-GC-MS, and SPME-GC-MS. *Talanta* **2021**, *221*, 121450. [CrossRef]
5. Guimarães, L.F.L.; da Silva, M.Z.F.; do Nascimento, R.F.; Alcântara, D.B. Method Validation and Determination of Ametryn Pesticide in Water Samples by QuEChERS-GC-MS. *Chemosensors* **2025**, *13*, 103. [CrossRef]
6. Feng, W.; Deng, Y.; Yang, F.; Miao, Q.; Ngien, S.K. Systematic Review of Contaminants of Emerging Concern (CECs): Distribution, Risks, and Implications for Water Quality and Health. *Water* **2023**, *15*, 3922. [CrossRef]
7. Lazofsky, A.; Buckley, B. Recent Trends in Multiclass Analysis of Emerging Endocrine Disrupting Contaminants (EDCs) in Drinking Water. *Molecules* **2022**, *27*, 8835. [CrossRef] [PubMed]
8. Wang, M.; Xu, Y.; Xie, Y.; Yang, L.; Zhang, J. A Review of the Sources, Monitoring, Detection, and Removal of Typical Olfactory Substances Geosmin and 2-Methylisoborneol. *Water* **2025**, *17*, 1236. [CrossRef]
9. Kumar, M.; Sridharan, S.; Sawarkar, A.D.; Shakeel, A.; Anerao, P.; Mannina, G.; Sharma, P.; Pandey, A. Current Research Trends on Emerging Contaminants Pharmaceutical and Personal Care Products (PPCPs): A Comprehensive Review. *Sci. Total Environ.* **2023**, *859*, 160031. [CrossRef]
10. Schreiber, L.; Halko, R.; Santana-Viera, S.; Michalides, N.M.; Sosa-Ferrera, Z.; Santana-Rodríguez, J.J. Evaluation of European Watch List Contaminants in Environmental Matrices and Microplastics: Analytical Strategies, Mechanisms of Adsorption and Occurrence. *Trends Environ. Anal. Chem.* **2024**, *44*, e00245. [CrossRef]
11. Ranjan Maji, S.; Roy, C.; Kumar Sinha, S. Gas Chromatography–Mass Spectrometry (GC-MS): A Comprehensive Review of Synergistic Combinations and Their Applications in the Past Two Decades. *J. Anal. Sci. Appl. Biotechnol.* **2023**, *5*, 72–85. [CrossRef]
12. Santos, F.J.; Galceran, M.T. Modern Developments in Gas Chromatography–Mass Spectrometry-Based Environmental Analysis. *J. Chromatogr. A* **2003**, *1000*, 125–151. [CrossRef]
13. Nika, M.-C.; Alygizakis, N.; Arvaniti, O.S.; Thomaidis, N.S. Non-Target Screening of Emerging Contaminants in Landfills: A Review. *Curr. Opin. Environ. Sci. Health* **2023**, *32*, 100430. [CrossRef]
14. Smith, D.; Španěl, P.; Demarais, N.; Langford, V.S.; McEwan, M.J. Recent Developments and Applications of Selected Ion Flow Tube Mass Spectrometry (SIFT-MS). *Mass. Spectrom. Rev.* **2025**, *44*, 101–134. [CrossRef]
15. Jia, W.; Liu, H.; Ma, Y.; Huang, G.; Liu, Y.; Zhao, B.; Xie, D.; Huang, K.; Wang, R. Reproducibility in Nontarget Screening (NTS) of Environmental Emerging Contaminants: Assessing Different HLB SPE Cartridges and Instruments. *Sci. Total Environ.* **2024**, *912*, 168971. [CrossRef]
16. Duff, D.; Lennard, C.; Li, Y.; Doyle, C.; Edge, K.J.; Holland, I.; Lothridge, K.; Johnstone, P.; Beylerian, P.; Spikmans, V. Portable Gas Chromatography–Mass Spectrometry Method for the in-Field Screening of Organic Pollutants in Soil and Water at Pollution Incidents. *Environ. Sci. Pollut. Res.* **2023**, *30*, 93088–93102. [CrossRef]
17. Ieda, T.; Hashimoto, S. GC × GC and Computational Strategies for Detecting and Analyzing Environmental Contaminants. *TrAC Trends Anal. Chem.* **2023**, *165*, 117118. [CrossRef]
18. Cairoli, M.; Van Den Doel, A.; Postma, B.; Offermans, T.; Zemmelink, H.; Stroomberg, G.; Buydens, L.; Van Kollenburg, G.; Jansen, J. Monitoring Pollution Pathways in River Water by Predictive Path Modelling Using Untargeted GC-MS Measurements. *npj Clean. Water* **2023**, *6*, 48. [CrossRef]
19. Lübeck, J.S.; Alexandrino, G.L.; Christensen, J.H. GC × GC–HRMS Nontarget Fingerprinting of Organic Micropollutants in Urban Freshwater Sediments. *Environ. Sci. Eur.* **2020**, *32*, 78. [CrossRef]
20. Zaid, A.; Hassan, N.H.; Marriott, P.J.; Wong, Y.F. Comprehensive Two-Dimensional Gas Chromatography as a Bioanalytical Platform for Drug Discovery and Analysis. *Pharmaceutics* **2023**, *15*, 1121. [CrossRef] [PubMed]
21. Acharya, S.; Sharmin, R.S.; Fiutowski, J.; Mishra, Y.K.; De Oliveira Hansen, R. Sensing Volatile Organic Compounds in Aquatic Samples: A Review. *Water Supply* **2024**, *24*, 3314–3325. [CrossRef]

22. Zhang, Q.; Xu, H.; Song, N.; Liu, S.; Wang, Y.; Ye, F.; Ju, Y.; Jiao, S.; Shi, L. New Insight into Fate and Transport of Organic Compounds from Pollution Sources to Aquatic Environment Using Non-Targeted Screening: A Wastewater Treatment Plant Case Study. *Sci. Total Environ.* **2023**, *863*, 161031. [CrossRef]
23. Liberatore, N.; Felizzato, G.; Mengali, S.; Viola, R.; Romolo, F.S. A Novel Signal Processing Approach Enabled by Machine Learning for the Detection and Identification of Chemical Warfare Agent Simulants Using a GC-QEPAS System. *Forensic Sci. Res.* **2025**, *10*, owaf002. [CrossRef]
24. Feizi, N.; Hashemi-Nasab, F.S.; Golpelichi, F.; Saburouh, N.; Parastar, H. Recent Trends in Application of Chemometric Methods for GC-MS and GC × GC-MS-Based Metabolomic Studies. *TrAC Trends Anal. Chem.* **2021**, *138*, 116239. [CrossRef]
25. Huang, T.-Y.; Chung Yu, J.C. Assessment of Artificial Intelligence to Detect Gasoline in Fire Debris Using HS-SPME-GC/MS and Transfer Learning. *J. Forensic Sci.* **2024**, *69*, 1222–1234. [CrossRef]
26. Baccolo, G.; Quintanilla-Casas, B.; Vichi, S.; Augustijn, D.; Bro, R. From Untargeted Chemical Profiling to Peak Tables—A Fully Automated AI Driven Approach to Untargeted GC-MS. *TrAC Trends Anal. Chem.* **2021**, *145*, 116451. [CrossRef]
27. Niarchos, G.; Alygizakis, N.; Carere, M.; Dulio, V.; Engwall, M.; Hyötyläinen, T.; Kallenborn, R.; Karakitsios, S.; Karakoltzidis, A.; Kärrman, A.; et al. Pioneering an Effect-Based Early Warning System for Hazardous Chemicals in the Environment. *TrAC Trends Anal. Chem.* **2024**, *180*, 117901. [CrossRef]
28. Catarro, G.; Pelixo, R.; Feijó, M.; Rosado, T.; Socorro, S.; Araújo, A.R.T.S.; Gallardo, E. Analytical Approaches Using GC-MS for the Detection of Pollutants in Wastewater Towards Environmental and Human Health Benefits: A Comprehensive Review. *Chemosensors* **2025**, *13*, 253. [CrossRef]
29. Licen, S.; Muzic, E.; Briguglio, S.; Tolloi, A.; Barbieri, P.; Giungato, P. Derivatized Volatile Organic Compound Characterization of Friulano Wine from Collio (Italy–Slovenia) by HS-SPME-GC-MS and Discrimination from Other Varieties by Chemometrics. *Br. Food J.* **2021**, *123*, 2844–2855. [CrossRef]
30. Wong, S.L.; Ng, L.T.; Tan, J.; Pan, J. Screening Unknown Novel Psychoactive Substances Using GC–MS Based Machine Learning. *Forensic Chem.* **2023**, *34*, 100499. [CrossRef]
31. Nie, W.; Alimujiang, S.; Zhang, Y.; Zhang, S.; Li, W. A Multi-Omics Approach Combining GC-MS, LC-MS, and FT-NIR with Chemometrics and Machine Learning for Metabolites Systematic Profiling and Geographical Origin Tracing of *Artemisia Argyi Folium*. *J. Chromatogr. A* **2025**, *1757*, 466138. [CrossRef]
32. Gan, Y.; Yang, T.; Gu, W.; Guo, L.; Qiu, R.; Wang, S.; Zhang, Y.; Tang, M.; Yang, Z. Using HS-GC-MS and Flash GC e-Nose in Combination with Chemometric Analysis and Machine Learning Algorithms to Identify the Varieties, Geographical Origins and Production Modes of *Atractylodes lancea*. *Ind. Crops Prod.* **2024**, *209*, 117955. [CrossRef]
33. Herruzo-Ruiz, A.M.; Peralbo-Molina, Á.; López, C.-M.; Michán, C.; Alhama, J.; Chicano-Gálvez, E. Mass Spectrometry Imaging in Environmental Monitoring: From a Scarce Existing Past to a Promising Future. *Trends Environ. Anal. Chem.* **2024**, *42*, e00228. [CrossRef]
34. Wang, L.; Li, X.; Wang, Y.; Ren, X.; Liu, X.; Dong, Y.; Ma, J.; Song, R.; Wei, J.; Yu, A.; et al. Rapid Discrimination and Screening of Volatile Markers for Varietal Recognition of *Curcumae radix* Using ATR-FTIR and HS-GC-MS Combined with Chemometrics. *J. Ethnopharmacol.* **2021**, *280*, 114422. [CrossRef]
35. Song, K.; Guo, S.; Gong, Y.; Lv, D.; Wan, Z.; Zhang, Y.; Fu, Z.; Hu, K.; Lu, S. Non-Target Scanning of Organics from Cooking Emissions Using Comprehensive Two-Dimensional Gas Chromatography-Mass Spectrometer (GC × GC-MS). *Appl. Geochem.* **2023**, *151*, 105601. [CrossRef]
36. Petrick, L.M.; Shomron, N. AI/ML-Driven Advances in Untargeted Metabolomics and Exposomics for Biomedical Applications. *Cell Rep. Phys. Sci.* **2022**, *3*, 100978. [CrossRef]
37. Tufariello, M.; Pati, S.; Palombi, L.; Grieco, F.; Losito, I. Use of Multivariate Statistics in the Processing of Data on Wine Volatile Compounds Obtained by HS-SPME-GC-MS. *Foods* **2022**, *11*, 910. [CrossRef] [PubMed]
38. Lu, W.; Rankin, J.G.; Bondra, A.; Trader, C.; Heeren, A.; Harrington, P. de B. Ignitable Liquid Identification Using Gas Chromatography/Mass Spectrometry Data by Projected Difference Resolution Mapping and Fuzzy Rule-Building Expert System Classification. *Forensic Sci. Int.* **2012**, *220*, 210–218. [CrossRef]
39. Barea-Sepúlveda, M.; Duarte, H.; Aliaño-González, M.J.; Romano, A.; Medronho, B. Total Ion Chromatogram and Total Ion Mass Spectrum as Alternative Tools for Detection and Discrimination (A Review). *Chemosensors* **2022**, *10*, 465. [CrossRef]
40. Diera, T.; Thomsen, A.H.; Tisler, S.; Karlby, L.T.; Christensen, P.; Rosshaug, P.S.; Albrechtsen, H.-J.; Christensen, J.H. A Non-Target Screening Study of High-Density Polyethylene Pipes Revealed Rubber Compounds as Main Contaminant in a Drinking Water Distribution System. *Water Res.* **2023**, *229*, 119480. [CrossRef]
41. Mok, S.; Lee, S.; Choi, Y.; Jeon, J.; Kim, Y.H.; Moon, H.-B. Target and Non-Target Analyses of Neutral per- and Polyfluoroalkyl Substances from Fluorochemical Industries Using GC-MS/MS and GC-TOF: Insights on Their Environmental Fate. *Environ. Int.* **2023**, *182*, 108311. [CrossRef]

42. Mazur, D.M.; Detenchuk, E.A.; Sosnova, A.A.; Artaev, V.B.; Lebedev, A.T. GC-HRMS with Complementary Ionization Techniques for Target and Non-Target Screening for Chemical Exposure: Expanding the Insights of the Air Pollution Markers in Moscow Snow. *Sci. Total Environ.* **2021**, *761*, 144506. [CrossRef]
43. Dąbrowski, Ł. Non-Target Screening of Chemicals in Selected Cotton Products by GC/MS and Their Safety Assessment. *Molecules* **2024**, *29*, 3584. [CrossRef]
44. Wojnowski, W.; Kalinowska, K.; Majchrzak, T.; Zabiegała, B. Real-Time Monitoring of the Emission of Volatile Organic Compounds from Polylactide 3D Printing Filaments. *Sci. Total Environ.* **2022**, *805*, 150181. [CrossRef]
45. Meurs, J.; Sakkoula, E.; Cristescu, S.M. Real-Time Non-Invasive Monitoring of Short-Chain Fatty Acids in Exhaled Breath. *Front. Chem.* **2022**, *10*, 853541. [CrossRef] [PubMed]
46. Ma, X.-L.; Wang, X.-C.; Zhang, J.-N.; Liu, J.-N.; Ma, M.-H.; Ma, F.-L.; Lv, Y.; Yu, Y.-J.; She, Y. A Study of Flavor Variations during the Flaxseed Roasting Procedure by Developed Real-Time SPME GC–MS Coupled with Chemometrics. *Food Chem.* **2023**, *410*, 135453. [CrossRef] [PubMed]
47. Yang, X.; Wang, C.; Shao, H.; Zheng, Q. Non-Targeted Screening and Analysis of Volatile Organic Compounds in Drinking Water by DLLME with GC–MS. *Sci. Total Environ.* **2019**, *694*, 133494. [CrossRef]
48. Jirayupat, C.; Nagashima, K.; Hosomi, T.; Takahashi, T.; Tanaka, W.; Samransuksamer, B.; Zhang, G.; Liu, J.; Kanai, M.; Yanagida, T. Image Processing and Machine Learning for Automated Identification of Chemo-/Biomarkers in Chromatography–Mass Spectrometry. *Anal. Chem.* **2021**, *93*, 14708–14715. [CrossRef]
49. Izquierdo-Sandoval, D.; Sancho, J.V.; Hernández, F.; Portoles, T. Approaches for GC-HRMS Screening of Organic Microcontaminants: GC-APCI-IMS-QTOF versus GC-EI-QOrbitrap. *Environ. Sci. Technol.* **2025**, *59*, 2436–2448. [CrossRef] [PubMed]
50. Cho, J.; Lee, J.; Lim, C.-U.; Ahn, J. Quantification of Pesticides in Food Crops Using QuEChERS Approaches and GC-MS/MS. *Food Addit. Contam. Part A* **2016**, *33*, 1803–1816. [CrossRef]
51. Elmastas, A.; Umaz, A.; Pirinc, V.; Aydin, F. Quantitative Determination and Removal of Pesticide Residues in Fresh Vegetables and Fruit Products by LC–MS/MS and GC–MS/MS. *Environ. Monit. Assess.* **2023**, *195*, 277. [CrossRef]
52. Yıldırım, İ.; Çiftçi, U. Monitoring of Pesticide Residues in Peppers from Çanakkale (Turkey) Public Market Using QuEChERS Method and LC–MS/MS and GC–MS/MS Detection. *Environ. Monit. Assess.* **2022**, *194*, 570. [CrossRef]
53. Tsiantas, P.; Bempelou, E.; Doula, M.; Karasali, H. Validation and Simultaneous Monitoring of 311 Pesticide Residues in Loamy Sand Agricultural Soils by LC-MS/MS and GC-MS/MS, Combined with QuEChERS-Based Extraction. *Molecules* **2023**, *28*, 4268. [CrossRef]
54. Hakami, R.A.; Aqel, A.; Ghfar, A.A.; ALOthman, Z.A.; Badjah-Hadj-Ahmed, A.-Y. Development of QuEChERS Extraction Method for the Determination of Pesticide Residues in Cereals Using DART-ToF-MS and GC-MS Techniques. Correlation and Quantification Study. *J. Food Compos. Anal.* **2021**, *98*, 103822. [CrossRef]
55. Migowska, N.; Caban, M.; Stepnowski, P.; Kumirska, J. Simultaneous Analysis of Non-Steroidal Anti-Inflammatory Drugs and Estrogenic Hormones in Water and Wastewater Samples Using Gas Chromatography–Mass Spectrometry and Gas Chromatography with Electron Capture Detection. *Sci. Total Environ.* **2012**, *441*, 77–88. [CrossRef]
56. Gumbi, B.P.; Moodley, B.; Birungi, G.; Ndungu, P.G. Detection and Quantification of Acidic Drug Residues in South African Surface Water Using Gas Chromatography-Mass Spectrometry. *Chemosphere* **2017**, *168*, 1042–1050. [CrossRef]
57. Perin, M.; Dallegrave, A.; Suchecki Barnet, L.; Zanchetti Meneghini, L.; de Araújo Gomes, A.; Pizzolato, T.M. Pharmaceuticals, Pesticides and Metals/Metalloids in Lake Guaíba in Southern Brazil: Spatial and Temporal Evaluation and a Chemometrics Approach. *Sci. Total Environ.* **2021**, *793*, 148561. [CrossRef] [PubMed]
58. Santos, L.H.M.L.M.; Insa, S.; Arxé, M.; Buttiglieri, G.; Rodríguez-Mozaz, S.; Barceló, D. Analysis of Microplastics in the Environment: Identification and Quantification of Trace Levels of Common Types of Plastic Polymers Using Pyrolysis-GC/MS. *MethodsX* **2023**, *10*, 102143. [CrossRef] [PubMed]
59. Ishimura, T.; Iwai, I.; Matsui, K.; Mattonai, M.; Watanabe, A.; Robberson, W.; Cook, A.-M.; Allen, H.L.; Pipkin, W.; Teramae, N.; et al. Qualitative and Quantitative Analysis of Mixtures of Microplastics in the Presence of Calcium Carbonate by Pyrolysis-GC/MS. *J. Anal. Appl. Pyrolysis* **2021**, *157*, 105188. [CrossRef]
60. Garcia, M.A.; Liu, R.; Nihart, A.; El Hayek, E.; Castillo, E.; Barrozo, E.R.; Suter, M.A.; Bleske, B.; Scott, J.; Forsythe, K.; et al. Quantitation and Identification of Microplastics Accumulation in Human Placental Specimens Using Pyrolysis Gas Chromatography Mass Spectrometry. *Toxicol. Sci.* **2024**, *199*, 81–88. [CrossRef]
61. Leslie, H.A.; van Velzen, M.J.M.; Brandsma, S.H.; Vethaak, A.D.; Garcia-Vallejo, J.J.; Lamoree, M.H. Discovery and Quantification of Plastic Particle Pollution in Human Blood. *Environ. Int.* **2022**, *163*, 107199. [CrossRef]
62. Rauert, C.; Charlton, N.; Bagley, A.; Dunlop, S.A.; Symeonides, C.; Thomas, K.V. Assessing the Efficacy of Pyrolysis–Gas Chromatography–Mass Spectrometry for Nanoplastic and Microplastic Analysis in Human Blood. *Environ. Sci. Technol.* **2025**, *59*, 1984–1994. [CrossRef]

63. Feng, X.; Wang, H.; Wang, Z.; Huang, P.; Kan, J. Discrimination and Characterization of the Volatile Organic Compounds in Eight Kinds of Huajiao with Geographical Indication of China Using Electronic Nose, HS-GC-IMS and HS-SPME-GC–MS. *Food Chem.* **2022**, *375*, 131671. [CrossRef]
64. Nie, S.; Li, L.; Wang, Y.; Wu, Y.; Li, C.; Chen, S.; Zhao, Y.; Wang, D.; Xiang, H.; Wei, Y. Discrimination and Characterization of Volatile Organic Compound Fingerprints during Sea Bass (*Lateolabrax japonicas*) Fermentation by Combining GC-IMS and GC-MS. *Food Biosci.* **2022**, *50*, 102048. [CrossRef]
65. Bajo-Fernández, M.; Souza-Silva, É.A.; Barbas, C.; Rey-Stolle, M.F.; García, A. GC-MS-Based Metabolomics of Volatile Organic Compounds in Exhaled Breath: Applications in Health and Disease. A Review. *Front. Mol. Biosci.* **2024**, *10*, 1295955. [CrossRef]
66. Yuan, N.; Chi, X.; Ye, Q.; Liu, H.; Zheng, N. Analysis of Volatile Organic Compounds in Milk during Heat Treatment Based on E-Nose, E-Tongue and HS-SPME-GC-MS. *Foods* **2023**, *12*, 1071. [CrossRef]
67. Schanzmann, H.; Gaar, S.; Keip, S.; Telgheder, U.; Sielemann, S. Comparison of the Quantification Performance of Thermal Desorption GC-IMS and GC-MS in VOC Analysis. *Anal. Bioanal. Chem.* **2025**, *417*, 4179–4198. [CrossRef] [PubMed]
68. Vaye, O.; Ngumbu, R.S.; Xia, D. A Review of the Application of Comprehensive Two-Dimensional Gas Chromatography MS-Based Techniques for the Analysis of Persistent Organic Pollutants and Ultra-Trace Level of Organic Pollutants in Environmental Samples. *Rev. Anal. Chem.* **2022**, *41*, 63–73. [CrossRef]
69. Maurin, N.; Sayen, S.; Guillon, E. Gas Chromatography–Mass Spectrometry Analysis of Organic Pollutants in French Soils Irrigated with Agro-Industrial Wastewater. *Front. Environ. Sci.* **2023**, *11*, 1125487. [CrossRef]
70. Chowdhary, P.; Singh, A.; Chandra, R.; Kumar, P.S.; Raj, A.; Bharagava, R.N. Detection and Identification of Hazardous Organic Pollutants from Distillery Wastewater by GC-MS Analysis and Its Phytotoxicity and Genotoxicity Evaluation by Using *Allium cepa* and *Cicer arietinum* L. *Chemosphere* **2022**, *297*, 134123. [CrossRef]
71. Zhang, J.; Zhang, B.; Dong, J.; Tian, Y.; Lin, Y.; Fang, G.; Wang, S. Identification of Mouldy Rice Using an Electronic Nose Combined with SPME-GC/MS. *J. Stored Prod. Res.* **2022**, *95*, 101921. [CrossRef]
72. Chen, W.; Zou, Y.; Mo, W.; Di, D.; Wang, B.; Wu, M.; Huang, Z.; Hu, B. Onsite Identification and Spatial Distribution of Air Pollutants Using a Drone-Based Solid-Phase Microextraction Array Coupled with Portable Gas Chromatography-Mass Spectrometry via Continuous-Airflow Sampling. *Environ. Sci. Technol.* **2022**, *56*, 17100–17107. [CrossRef]
73. Vu-Duc, N.; Phung Thi, L.A.; Le-Minh, T.; Nguyen, L.-A.; Nguyen-Thi, H.; Pham-Thi, L.-H.; Doan-Thi, V.-A.; Le-Quang, H.; Nguyen-Xuan, H.; Thi Nguyen, T.; et al. Analysis of Polycyclic Aromatic Hydrocarbon in Airborne Particulate Matter Samples by Gas Chromatography in Combination with Tandem Mass Spectrometry (GC-MS/MS). *J. Anal. Methods Chem.* **2021**, *2021*, 6641326. [CrossRef] [PubMed]
74. Martinello, M.; Manzinello, C.; Dainese, N.; Giuliato, I.; Gallina, A.; Mutinelli, F. The Honey Bee: An Active Biosampler of Environmental Pollution and a Possible Warning Biomarker for Human Health. *Appl. Sci.* **2021**, *11*, 6481. [CrossRef]
75. Płotka-Wasylka, J.; Owczarek, K.; Namieśnik, J. Modern Solutions in the Field of Microextraction Using Liquid as a Medium of Extraction. *TrAC Trends Anal. Chem.* **2016**, *85*, 46–64. [CrossRef]
76. Płotka-Wasylka, J.; Szczepańska, N.; De La Guardia, M.; Namieśnik, J. Modern Trends in Solid Phase Extraction: New Sorbent Media. *TrAC Trends Anal. Chem.* **2016**, *77*, 23–43. [CrossRef]
77. Peñalver, R.; Ortiz, A.; Arroyo-Manzanares, N.; Campillo, N.; López-García, I.; Viñas, P. Non-Targeted Analysis by DLLME-GC-MS for the Monitoring of Pollutants in the Mar Menor Lagoon. *Chemosphere* **2022**, *286*, 131588. [CrossRef]
78. Tian, Y.; Liu, Y.; Dong, K.; Zhao, B.; Tang, S.; Nie, X.; Yan, Y. Advances in Rapid Detection of Volatile Organic Compounds (VOCs): From Conventional Techniques to Surface-Enhanced Raman Spectroscopy. *Results Chem.* **2025**, *16*, 102329. [CrossRef]
79. Pardina, D.; Santamaria, A.; Alonso, M.L.; Bartolomé, L.; Alonso, R.M.; Maña, J.A.; Bilbao, E.; Lombraña, J.I.; Bartolome, M.; Hernando, L.M. HS-SPME-GC/MS Method for the Simultaneous Determination of Trihalomethanes, Geosmin, and 2-Methylisoborneol in Water Samples. *Chemosensors* **2023**, *11*, 84. [CrossRef]
80. Ferracane, A.; Aloisi, I.; Galletta, M.; Zoccali, M.; Tranchida, P.Q.; Micalizzi, G.; Mondello, L. Automated Sample Preparation and Fast GC–MS Determination of Fatty Acids in Blood Samples and Dietary Supplements. *Anal. Bioanal. Chem.* **2022**, *414*, 8423–8435. [CrossRef] [PubMed]
81. Fan, X.; Xu, Z.; Zhang, H.; Liu, D.; Yang, Q.; Tao, Q.; Wen, M.; Kang, X.; Zhang, Z.; Lu, H. Fully Automatic Resolution of Untargeted GC-MS Data with Deep Learning Assistance. *Talanta* **2022**, *244*, 123415. [CrossRef] [PubMed]
82. Nam, S.L.; de la Mata, A.P.; Harynuk, J.J. Automated Screening and Filtering Scripts for GC × GC-TOFMS Metabolomics Data. *Separations* **2021**, *8*, 84. [CrossRef]
83. Kumar, R.; Parashar, A. Atomistic Simulations of Pristine and Nanoparticle Reinforced Hydrogels: A Review. *WIREs Comput. Mol. Sci.* **2023**, *13*, e1655. [CrossRef]
84. Bahraq, A.A.; Al-Osta, M.A.; Al-Amoudi, O.S.B.; Saleh, T.A.; Obot, I.B. Atomistic Simulation of Polymer-Cement Interactions: Progress and Research Challenges. *Constr. Build. Mater.* **2022**, *327*, 126881. [CrossRef]
85. Ward, L.; Wolverton, C. Atomistic Calculations and Materials Informatics: A Review. *Curr. Opin. Solid. State Mater. Sci.* **2017**, *21*, 167–176. [CrossRef]

86. Chen, Y.-Y.; Ross Kunz, M.; He, X.; Fushimi, R. Recent Progress toward Catalyst Properties, Performance, and Prediction with Data-Driven Methods. *Curr. Opin. Chem. Eng.* **2022**, *37*, 100843. [CrossRef]
87. Shambhawi; Mohan, O.; Choksi, T.S.; Lapkin, A.A. The Design and Optimization of Heterogeneous Catalysts Using Computational Methods. *Catal. Sci. Technol.* **2024**, *14*, 515–532. [CrossRef]
88. Thomas, R.; Mary, Y.S.; Resmi, K.S.; Narayana, B.; Sarojini, S.B.K.; Armaković, S.; Armaković, S.J.; Vijayakumar, G.; Alsenoy, C.V.; Mohan, B.J. Synthesis and Spectroscopic Study of Two New Pyrazole Derivatives with Detailed Computational Evaluation of Their Reactivity and Pharmaceutical Potential. *J. Mol. Struct.* **2019**, *1181*, 599–612. [CrossRef]
89. Haruna, K.; Kumar, V.S.; Armaković, S.J.; Armaković, S.; Mary, Y.S.; Thomas, R.; Popoola, S.A.; Almohammedi, A.R.; Roxy, M.S.; Al-Saadi, A.A. Spectral Characterization, Thermochemical Studies, Periodic SAPT Calculations and Detailed Quantum Mechanical Profiling Various Physico-Chemical Properties of 3,4-Dichlorodiuron. *Spectrochim. Acta Part A Mol. Biomol. Spectrosc.* **2020**, *228*, 117580. [CrossRef] [PubMed]
90. Bielenica, A.; Beegum, S.; Mary, Y.S.; Mary, Y.S.; Thomas, R.; Armaković, S.; Armaković, S.J.; Madeddu, S.; Struga, M.; Van Alsenoy, C. Experimental and Computational Analysis of 1-(4-Chloro-3-Nitrophenyl)-3-(3,4-Dichlorophenyl)Thiourea. *J. Mol. Struct.* **2020**, *1205*, 127587. [CrossRef]
91. Aghdasi, P.; Yousefi, S.; Ansari, R. A DFT Investigation on the Mechanical and Structural Properties of Halogen- and Metal-Adsorbed Silicene Nanosheets. *Mater. Chem. Phys.* **2022**, *283*, 126029. [CrossRef]
92. El-Sayed, D.S. Electronic Band Structure and Density of State Modulation of Amphetamine and ABW Type–Zeolite Adsorption System: DFT-CASTEP Analysis. *J. Mol. Model.* **2023**, *29*, 96. [CrossRef]
93. Bai, Z.; Lan, M.; Yu, W.; Shen, S. Predicting Strain Effects on Adsorption Energy Based on Atomistic Structure and Density of States. *Int. J. Mech. Sci.* **2025**, *294*, 110234. [CrossRef]
94. Yang, B.; Uphoff, M.; Zhang, Y.-Q.; Reichert, J.; Seitsonen, A.P.; Bauer, A.; Pfleiderer, C.; Barth, J.V. Atomistic Investigation of Surface Characteristics and Electronic Features at High-Purity FeSi(110) Presenting Interfacial Metallicity. *Proc. Natl. Acad. Sci. USA* **2021**, *118*, e2021203118. [CrossRef]
95. Gomez, H.; Groves, M.N.; Neupane, M.R. Study of the Structural Phase Transition in Diamond (100) & (111) Surfaces. *Carbon. Trends* **2021**, *3*, 100033. [CrossRef]
96. Stampelou, M.; Ladds, G.; Kolocouris, A. Computational Workflow for Refining AlphaFold Models in Drug Design Using Kinetic and Thermodynamic Binding Calculations: A Case Study for the Unresolved Inactive Human Adenosine A3 Receptor. *J. Phys. Chem. B* **2024**, *128*, 914–936. [CrossRef]
97. Sellner, M.; Fischer, A.; Don, C.G.; Smieško, M. Conformational Landscape of Cytochrome P450 Reductase Interactions. *Int. J. Mol. Sci.* **2021**, *22*, 1023. [CrossRef]
98. Friedman, R. Computational Studies of Protein–Drug Binding Affinity Changes upon Mutations in the Drug Target. *WIREs Comput. Mol. Sci.* **2022**, *12*, e1563. [CrossRef]
99. Chu, W.-T.; Yan, Z.; Chu, X.; Zheng, X.; Liu, Z.; Xu, L.; Zhang, K.; Wang, J. Physics of Biomolecular Recognition and Conformational Dynamics. *Rep. Prog. Phys.* **2021**, *84*, 126601. [CrossRef]
100. Mishra, S.B.; Marutheeswaran, S.; Roy, S.C.; Natarajan, V.; Rai, P.K.; Nanda, B.R.K. Adsorption and Degradation Mechanism of 2,4,6-Trinitrotoluene on TiO_2 (110) Surface. *Surf. Sci.* **2021**, *713*, 121902. [CrossRef]
101. Shen, L.; Yu, X.; Li, M.; Deng, S.; Cao, H. The In-Situ Generation of ClO• by Single- and Dual-Atom Catalysis of Chloride Ions to Degrade Sulfonamide Antibiotics: A DFT Study. *Chem. Eng. J.* **2024**, *485*, 149719. [CrossRef]
102. Ma, Q.; Ming, J.; Sun, X.; Zhang, H.; An, G.; Kawazoe, N.; Chen, G.; Yang, Y. Photocatalytic Degradation of Multiple-Organic-Pollutant under Visible Light by Graphene Oxide Modified Composite: Degradation Pathway, DFT Calculation and Mechanism. *J. Environ. Manag.* **2023**, *347*, 119128. [CrossRef] [PubMed]
103. Shen, Y.; Yang, J.; Zhu, C.; Fang, Q.; Song, S.; Chen, B. Mechanistic Insights into the Atomic Distance Effect on Adsorption and Degradation of Aromatic Compounds. *ACS Catal.* **2023**, *13*, 8943–8954. [CrossRef]
104. Zhang, J.; Liu, C.; Wu, Y.; Li, X.; Zhang, J.; Liang, J.; Li, Y. Adsorption of Tetracycline by Polycationic Straw: Density Functional Theory Calculation for Mechanism and Machine Learning Prediction for Tetracyclines' Remediation. *Environ. Pollut.* **2024**, *340*, 122869. [CrossRef]
105. Zhao, C.; Zhang, J.; Zhang, W.; Yang, Y.; Guo, D.; Zhang, H.; Liu, L. Reveal the Main Factors and Adsorption Behavior Influencing the Adsorption of Pollutants on Natural Mineral Adsorbents: Based on Machine Learning Modeling and DFT Calculation. *Sep. Purif. Technol.* **2024**, *331*, 125706. [CrossRef]
106. Lyshchuk, H.; Verkhovtsev, A.V.; Kočišek, J.; Fedor, J.; Solov'yov, A.V. Release of Neutrals in Electron-Induced Ligand Separation from MeCpPtMe3: Theory Meets Experiment. *J. Phys. Chem. A* **2025**, *129*, 2016–2023. [CrossRef]
107. Kurzydym, I.; Błaziak, A.; Podgórniak, K.; Kułacz, K.; Błaziak, K. Mechanistic Insight into the Kinetic Fragmentation of Norpinonic Acid in the Gas Phase: An Experimental and Density Functional Theory (DFT) Study. *Atmos. Chem. Phys.* **2024**, *24*, 9309–9322. [CrossRef]

108. Eskandari, M.; Faraz, S.M.; Hosseini, S.E.; Moradi, S.; Saeidian, H. Electron Ionization Mass Spectrometry Fragmentation Routes of Chemical Weapons Convention-Related Organoarsenic Compounds: Electron Ionization and Density Functional Theory Studies. *Rapid Commun. Mass. Spectrom.* **2023**, *37*, e9511. [CrossRef]
109. Sandoval-Pauker, C.; Yin, S.; Castillo, A.; Ocuane, N.; Puerto-Diaz, D.; Villagrán, D. Computational Chemistry as Applied in Environmental Research: Opportunities and Challenges. *ACS EST Eng.* **2024**, *4*, 66–95. [CrossRef]
110. Armaković, S.J.; Armaković, S.; Savanović, M.M. Photocatalytic Application of Polymers in Removing Pharmaceuticals from Water: A Comprehensive Review. *Catalysts* **2024**, *14*, 447. [CrossRef]
111. Stephens, P.J.; Devlin, F.J.; Chabalowski, C.F.; Frisch, M.J. Ab Initio Calculation of Vibrational Absorption and Circular Dichroism Spectra Using Density Functional Force Fields. *J. Phys. Chem.* **1994**, *98*, 11623–11627. [CrossRef]
112. Vosko, S.H.; Wilk, L.; Nusair, M. Accurate Spin-Dependent Electron Liquid Correlation Energies for Local Spin Density Calculations: A Critical Analysis. *Can. J. Phys.* **1980**, *58*, 1200–1211. [CrossRef]
113. Lee, C.; Yang, W.; Parr, R.G. Development of the Colle-Salvetti Correlation-Energy Formula into a Functional of the Electron Density. *Phys. Rev. B* **1988**, *37*, 785. [CrossRef]
114. Becke, A.D. Density-functional Thermochemistry. III. The Role of Exact Exchange. *J. Chem. Phys.* **1993**, *98*, 5648–5652. [CrossRef]
115. Perdew, J.P.; Burke, K.; Ernzerhof, M. Generalized Gradient Approximation Made Simple. *Phys. Rev. Lett.* **1996**, *77*, 3865–3868. [CrossRef] [PubMed]
116. Perdew, J.P.; Burke, K.; Ernzerhof, M. Generalized Gradient Approximation Made Simple [Phys. Rev. Lett. 77, 3865 (1996)]. *Phys. Rev. Lett.* **1997**, *78*, 1396. [CrossRef]
117. Zhao, Y.; Truhlar, D.G. Density Functionals with Broad Applicability in Chemistry. *Acc. Chem. Res.* **2008**, *41*, 157–167. [CrossRef]
118. Valero, R.; Costa, R.; Moreira, I.d.P.R.; Truhlar, D.G.; Illas, F. Performance of the M06 Family of Exchange-Correlation Functionals for Predicting Magnetic Coupling in Organic and Inorganic Molecules. *J. Chem. Phys.* **2008**, *128*, 114103. [CrossRef]
119. Jacquemin, D.; Perpète, E.A.; Ciofini, I.; Adamo, C.; Valero, R.; Zhao, Y.; Truhlar, D.G. On the Performances of the M06 Family of Density Functionals for Electronic Excitation Energies. *J. Chem. Theory Comput.* **2010**, *6*, 2071–2085. [CrossRef] [PubMed]
120. Zhao, Y.; Truhlar, D.G. The M06 Suite of Density Functionals for Main Group Thermochemistry, Thermochemical Kinetics, Noncovalent Interactions, Excited States, and Transition Elements: Two New Functionals and Systematic Testing of Four M06-Class Functionals and 12 Other Functionals. *Theor. Chem. Acc.* **2008**, *120*, 215–241. [CrossRef]
121. Chai, J.-D.; Head-Gordon, M. Systematic Optimization of Long-Range Corrected Hybrid Density Functionals. *J. Chem. Phys.* **2008**, *128*, 084106. [CrossRef]
122. Chai, J.-D.; Head-Gordon, M. Long-Range Corrected Hybrid Density Functionals with Damped Atom–Atom Dispersion Corrections. *Phys. Chem. Chem. Phys.* **2008**, *10*, 6615–6620. [CrossRef]
123. Bannwarth, C.; Caldeweyher, E.; Ehlert, S.; Hansen, A.; Pracht, P.; Seibert, J.; Spicher, S.; Grimme, S. Extended Tight-Binding Quantum Chemistry Methods. *WIREs Comput. Mol. Sci.* **2021**, *11*, e1493. [CrossRef]
124. Dral, P.O.; Zubatiuk, T. Chapter 24—Improving Semiempirical Quantum Mechanical Methods with Machine Learning. In *Quantum Chemistry in the Age of Machine Learning*; Dral, P.O., Ed.; Elsevier: Amsterdam, The Netherlands, 2023; pp. 559–575, ISBN 978-0-323-90049-2.
125. Dral, P.O.; Řezáč, J. Chapter 3—Semiempirical Quantum Mechanical Methods. In *Quantum Chemistry in the Age of Machine Learning*; Dral, P.O., Ed.; Elsevier: Amsterdam, The Netherlands, 2023; pp. 67–92, ISBN 978-0-323-90049-2.
126. Stewart, J.J.P. Optimization of Parameters for Semiempirical Methods IV: Extension of MNDO, AM1, and PM3 to More Main Group Elements. *J. Mol. Model.* **2004**, *10*, 155–164. [CrossRef]
127. Stewart, J.J.P. Optimization of Parameters for Semiempirical Methods II. Applications. *J. Comput. Chem.* **1989**, *10*, 221–264. [CrossRef]
128. Stewart, J.J.P. Optimization of Parameters for Semiempirical Methods I. Method. *J. Comput. Chem.* **1989**, *10*, 209–220. [CrossRef]
129. Stewart, J.J.P. Optimization of Parameters for Semiempirical Methods VI: More Modifications to the NDDO Approximations and Re-Optimization of Parameters. *J. Mol. Model.* **2013**, *19*, 1–32. [CrossRef]
130. Köhler, C.; Seifert, G.; Frauenheim, T. Density Functional Based Calculations for Fen ($n \leq 32$). *Chem. Phys.* **2005**, *309*, 23–31. [CrossRef]
131. Elstner, M.; Porezag, D.; Jungnickel, G.; Elsner, J.; Haugk, M.; Frauenheim, T.; Suhai, S.; Seifert, G. Self-Consistent-Charge Density-Functional Tight-Binding Method for Simulations of Complex Materials Properties. *Phys. Rev. B* **1998**, *58*, 7260–7268. [CrossRef]
132. Seifert, G.; Porezag, D.; Frauenheim, T. Calculations of Molecules, Clusters, and Solids with a Simplified LCAO-DFT-LDA Scheme. *Int. J. Quantum Chem.* **1996**, *58*, 185–192. [CrossRef]
133. Porezag, D.; Frauenheim, T.; Köhler, T.; Seifert, G.; Kaschner, R. Construction of Tight-Binding-like Potentials on the Basis of Density-Functional Theory: Application to Carbon. *Phys. Rev. B* **1995**, *51*, 12947–12957. [CrossRef]
134. Ehlert, S.; Stahn, M.; Spicher, S.; Grimme, S. Robust and Efficient Implicit Solvation Model for Fast Semiempirical Methods. *J. Chem. Theory Comput.* **2021**, *17*, 4250–4261. [CrossRef]

135. Bannwarth, C.; Ehlert, S.; Grimme, S. GFN2-xTB—An Accurate and Broadly Parametrized Self-Consistent Tight-Binding Quantum Chemical Method with Multipole Electrostatics and Density-Dependent Dispersion Contributions. *J. Chem. Theory Comput.* **2019**, *15*, 1652–1671. [CrossRef]
136. Grimme, S.; Bannwarth, C.; Shushkov, P. A Robust and Accurate Tight-Binding Quantum Chemical Method for Structures, Vibrational Frequencies, and Noncovalent Interactions of Large Molecular Systems Parametrized for All Spd-Block Elements (Z = 1–86). *J. Chem. Theory Comput.* **2017**, *13*, 1989–2009. [CrossRef] [PubMed]
137. Spicher, S.; Grimme, S. Robust Atomistic Modeling of Materials, Organometallic, and Biochemical Systems. *Angew. Chem. Int. Ed.* **2020**, *59*, 15665–15673. [CrossRef] [PubMed]
138. Neese, F. Software Update: The ORCA Program System—Version 5.0. *WIREs Comput. Mol. Sci.* **2022**, *12*, e1606. [CrossRef]
139. Vreven, T.; Byun, K.S.; Komáromi, I.; Dapprich, S.; Montgomery, J.A., Jr.; Morokuma, K.; Frisch, M.J. Combining Quantum Mechanics Methods with Molecular Mechanics Methods in ONIOM. *J. Chem. Theory Comput.* **2006**, *2*, 815–826. [CrossRef]
140. Bhattacharyya, S.; Poi, R.; Baskey Sen, M.; Mandal, S.; Hazra, D.K.; Karmakar, R. Efficient Fabrication of pH-Modified Graphene Nano-Adsorbent for Effective Determination and Monitoring of Multi-Class Pesticide Residues in Market-Fresh Vegetables by GC-MS. *J. Food Compos. Anal.* **2023**, *118*, 105153. [CrossRef]
141. Riyaz, M.; Goel, N. A QM/MM Study to Investigate Selectivity of Nanoporous Graphene Membrane for Arsenate and Chromate Removal from Water. *Chem. Phys. Lett.* **2017**, *685*, 371–376. [CrossRef]
142. Mollaamin, F.; Monajjemi, M. Graphene Embedded with Transition Metals for Capturing Carbon Dioxide: Gas Detection Study Using QM Methods. *Clean. Technol.* **2023**, *5*, 403–417. [CrossRef]
143. Turney, J.M.; Simmonett, A.C.; Parrish, R.M.; Hohenstein, E.G.; Evangelista, F.A.; Fermann, J.T.; Mintz, B.J.; Burns, L.A.; Wilke, J.J.; Abrams, M.L.; et al. Psi4: An Open-Source Ab Initio Electronic Structure Program. *WIREs Comput. Mol. Sci.* **2012**, *2*, 556–565. [CrossRef]
144. Parrish, R.M.; Burns, L.A.; Smith, D.G.A.; Simmonett, A.C.; DePrince, A.E.I.; Hohenstein, E.G.; Bozkaya, U.; Sokolov, A.Y.; Di Remigio, R.; Richard, R.M.; et al. Psi4 1.1: An Open-Source Electronic Structure Program Emphasizing Automation, Advanced Libraries, and Interoperability. *J. Chem. Theory Comput.* **2017**, *13*, 3185–3197. [CrossRef]
145. Smith, D.G.A.; Burns, L.A.; Simmonett, A.C.; Parrish, R.M.; Schieber, M.C.; Galvelis, R.; Kraus, P.; Kruse, H.; Di Remigio, R.; Alenaizan, A.; et al. PSI4 1.4: Open-Source Software for High-Throughput Quantum Chemistry. *J. Chem. Phys.* **2020**, *152*, 184108. [CrossRef]
146. Lu, T. A Comprehensive Electron Wavefunction Analysis Toolbox for Chemists, Multiwfn. *J. Chem. Phys.* **2024**, *161*, 082503. [CrossRef] [PubMed]
147. Lu, T.; Chen, Q. Van Der Waals Potential: An Important Complement to Molecular Electrostatic Potential in Studying Intermolecular Interactions. *J. Mol. Model.* **2020**, *26*, 315. [CrossRef] [PubMed]
148. Lu, T.; Manzetti, S. Wavefunction and Reactivity Study of Benzo[a]Pyrene Diol Epoxide and Its Enantiomeric Forms. *Struct Chem* **2014**, *25*, 1521–1533. [CrossRef]
149. Lu, T.; Chen, F. Multiwfn: A Multifunctional Wavefunction Analyzer. *J. Comput. Chem.* **2012**, *33*, 580–592. [CrossRef] [PubMed]
150. Froitzheim, T.; Müller, M.; Hansen, A.; Grimme, S. G-xTB: A General-Purpose Extended Tight-Binding Electronic Structure Method For the Elements H to Lr (Z=1–103). *ChemRxiv* **2025**. [CrossRef]
151. Plimpton, S. Fast Parallel Algorithms for Short-Range Molecular Dynamics. *J. Comput. Phys.* **1995**, *117*, 1–19. [CrossRef]
152. Thompson, A.P.; Aktulga, H.M.; Berger, R.; Bolintineanu, D.S.; Brown, W.M.; Crozier, P.S.; in 't Veld, P.J.; Kohlmeyer, A.; Moore, S.G.; Nguyen, T.D.; et al. LAMMPS—A Flexible Simulation Tool for Particle-Based Materials Modeling at the Atomic, Meso, and Continuum Scales. *Comput. Phys. Commun.* **2022**, *271*, 108171. [CrossRef]
153. Páll, S.; Abraham, M.J.; Kutzner, C.; Hess, B.; Lindahl, E. Tackling Exascale Software Challenges in Molecular Dynamics Simulations with GROMACS. In Proceedings of the Solving Software Challenges for Exascale, EASC 2014, Stockholm, Sweden, 2–3 April 2014; Markidis, S., Laure, E., Eds.; Springer: Cham, Switzerland, 2015; pp. 3–27.
154. Bekker, H.; Berendsen, H.; Dijkstra, E.; Achterop, S.; Vondrumen, R.; Vanderspoel, D.; Sijbers, A.; Keegstra, H.; Renardus, M. Gromacs—A Parallel Computer for Molecular-Dynamics Simulations. In Proceedings of the 4th International Conference on Computational Physics (PC 92), Prague, Czech Republic, 24–28 August 1992; World Scientific Publishing: Singapore, 1993; pp. 252–256.
155. Abraham, M.J.; Murtola, T.; Schulz, R.; Páll, S.; Smith, J.C.; Hess, B.; Lindahl, E. GROMACS: High Performance Molecular Simulations through Multi-Level Parallelism from Laptops to Supercomputers. *SoftwareX* **2015**, *1–2*, 19–25. [CrossRef]
156. Pronk, S.; Páll, S.; Schulz, R.; Larsson, P.; Bjelkmar, P.; Apostolov, R.; Shirts, M.R.; Smith, J.C.; Kasson, P.M.; van der Spoel, D.; et al. GROMACS 4.5: A High-Throughput and Highly Parallel Open Source Molecular Simulation Toolkit. *Bioinformatics* **2013**, *29*, 845–854. [CrossRef]
157. Hess, B.; Kutzner, C.; van der Spoel, D.; Lindahl, E. GROMACS 4: Algorithms for Highly Efficient, Load-Balanced, and Scalable Molecular Simulation. *J. Chem. Theory Comput.* **2008**, *4*, 435–447. [CrossRef]

158. Van Der Spoel, D.; Lindahl, E.; Hess, B.; Groenhof, G.; Mark, A.E.; Berendsen, H.J.C. GROMACS: Fast, Flexible, and Free. *J. Comput. Chem.* **2005**, *26*, 1701–1718. [CrossRef]
159. Lindahl, E.; Hess, B.; Van Der Spoel, D. GROMACS 3.0: A Package for Molecular Simulation and Trajectory Analysis. *J. Mol. Model.* **2001**, *7*, 306–317. [CrossRef]
160. Berendsen, H.J.C.; van der Spoel, D.; van Drunen, R. GROMACS: A Message-Passing Parallel Molecular Dynamics Implementation. *Comput. Phys. Commun.* **1995**, *91*, 43–56. [CrossRef]
161. Sohrabi, S.; Rahimi, P.; Khedri, M.; Heydari, R.; Mirzaei, M.; Bahrami, A.; Akhlaghian, F.; Taghipoor, M. Evaluation of Machine Learning and Molecular Dynamics Models for Photocatalytic Water Decontamination. *Process Saf. Environ. Prot.* **2025**, *195*, 106780. [CrossRef]
162. Neese, F.; Wennmohs, F.; Becker, U.; Riplinger, C. The ORCA Quantum Chemistry Program Package. *J. Chem. Phys.* **2020**, *152*, 224108. [CrossRef]
163. Neese, F. The ORCA Program System. *WIREs Comput. Mol. Sci.* **2012**, *2*, 73–78. [CrossRef]
164. Neese, F. Software Update: The ORCA Program System, Version 4.0. *WIREs Comput. Mol. Sci.* **2018**, *8*, e1327. [CrossRef]
165. Neese, F.; Wennmohs, F.; Hansen, A.; Becker, U. Efficient, Approximate and Parallel Hartree–Fock and Hybrid DFT Calculations. A 'Chain-of-Spheres' Algorithm for the Hartree–Fock Exchange. *Chem. Phys.* **2009**, *356*, 98–109. [CrossRef]
166. Teale, A.M.; Helgaker, T.; Savin, A.; Adamo, C.; Aradi, B.; Arbuznikov, A.V.; Ayers, P.W.; Baerends, E.J.; Barone, V.; Calaminici, P.; et al. DFT Exchange: Sharing Perspectives on the Workhorse of Quantum Chemistry and Materials Science. *Phys. Chem. Chem. Phys.* **2022**, *24*, 28700–28781. [CrossRef]
167. Neese, F. The SHARK Integral Generation and Digestion System. *J. Comput. Chem.* **2022**, *44*, 381–396. [CrossRef] [PubMed]
168. Guo, Y.; Riplinger, C.; Liakos, D.G.; Becker, U.; Saitow, M.; Neese, F. Linear Scaling Perturbative Triples Correction Approximations for Open-Shell Domain-Based Local Pair Natural Orbital Coupled Cluster Singles and Doubles Theory [DLPNO-CCSD(T0/T)]. *J. Chem. Phys.* **2020**, *152*, 024116. [CrossRef] [PubMed]
169. Liakos, D.G.; Guo, Y.; Neese, F. Comprehensive Benchmark Results for the Domain Based Local Pair Natural Orbital Coupled Cluster Method (DLPNO-CCSD(T)) for Closed- and Open-Shell Systems. *J. Phys. Chem. A* **2020**, *124*, 90–100. [CrossRef] [PubMed]
170. Armaković, S.; Armaković, S.J. Predicting Properties of Imidazolium-Based Ionic Liquids via Atomistica Online: Machine Learning Models and Web Tools. *Computation* **2025**, *13*, 216. [CrossRef]
171. Armaković, S.; Armaković, S.J. Atomistica.Online—Web Application for Generating Input Files for ORCA Molecular Modelling Package Made with the Anvil Platform. *Mol. Simul.* **2023**, *49*, 117–123. [CrossRef]
172. Armaković, S.; Armaković, S.J. Online and Desktop Graphical User Interfaces for Xtb Programme from Atomistica.Online Platform. *Mol. Simul.* **2024**, *50*, 560–570. [CrossRef]
173. Lu, T.; Chen, Q. Shermo: A General Code for Calculating Molecular Thermochemistry Properties. *Comput. Theor. Chem.* **2021**, *1200*, 113249. [CrossRef]
174. Landrum, G.; Tosco, P.; Kelley, B.; Rodriguez, R.; Cosgrove, D.; Vianello, R.; Sriniker; Gedeck, P.; Jones, G.; Kawashima, E.; et al. Rdkit/Rdkit: 2025_03_6 (Q1 2025) Release 2025. Available online: https://zenodo.org/records/15605628 (accessed on 1 August 2025).
175. Lienard, P.; Gavartin, J.; Boccardi, G.; Meunier, M. Predicting Drug Substances Autoxidation. *Pharm. Res.* **2015**, *32*, 300–310. [CrossRef]
176. Andersson, T.; Broo, A.; Evertsson, E. Prediction of Drug Candidates' Sensitivity Toward Autoxidation: Computational Estimation of C-H Dissociation Energies of Carbon-Centered Radicals. *J. Pharm. Sci.* **2014**, *103*, 1949–1955. [CrossRef] [PubMed]
177. Abraham, C.S.; Muthu, S.; Prasana, J.C.; Armaković, S.J.; Armaković, S.; Rizwana, F.; Ben Geoffrey, A.S. Spectroscopic Profiling (FT-IR, FT-Raman, NMR and UV-Vis), Autoxidation Mechanism (H-BDE) and Molecular Docking Investigation of 3-(4-Chlorophenyl)-N,N-Dimethyl-3-Pyridin-2-Ylpropan-1-Amine by DFT/TD-DFT and Molecular Dynamics: A Potential SSRI Drug. *Comput. Biol. Chem.* **2018**, *77*, 131–145. [CrossRef] [PubMed]
178. Khemalapure, S.S.; Katti, V.S.; Hiremath, C.S.; Basanagouda, M.; Hiremath, S.M.; Armaković, S.J.; Armaković, S. Molecular Structure, Optoelectronic Properties, Spectroscopic (FT-IR, FT-Raman and UV–Vis), H-BDE, NBO and Drug Likeness Investigations on 7, 8-Benzocoumarin-4-Acetic Acid (7BAA). *J. Mol. Struct.* **2019**, *1195*, 815–826. [CrossRef]
179. Shree Sowndarya, S.V.; Kim, Y.; Kim, S.; St. John, P.C.; Paton, R.S. Expansion of Bond Dissociation Prediction with Machine Learning to Medicinally and Environmentally Relevant Chemical Space. *Digit. Discov.* **2023**, *2*, 1900–1910. [CrossRef]
180. Wada, O.Z.; Olawade, D.B. Recent Occurrence of Pharmaceuticals in Freshwater, Emerging Treatment Technologies, and Future Considerations: A Review. *Chemosphere* **2025**, *374*, 144153. [CrossRef]
181. Tufail, A.; Price, W.E.; Mohseni, M.; Pramanik, B.K.; Hai, F.I. A Critical Review of Advanced Oxidation Processes for Emerging Trace Organic Contaminant Degradation: Mechanisms, Factors, Degradation Products, and Effluent Toxicity. *J. Water Process Eng.* **2021**, *40*, 101778. [CrossRef]

182. Rossomme, E.; Hart-Cooper, W.M.; Orts, W.J.; McMahan, C.M.; Head-Gordon, M. Computational Studies of Rubber Ozonation Explain the Effectiveness of 6PPD as an Antidegradant and the Mechanism of Its Quinone Formation. *Environ. Sci. Technol.* **2023**, *57*, 5216–5230. [CrossRef]
183. Li, T.; Song, Y.; Zhang, Z. DFT Study on the Mechanism of As(III) Oxidation in the Presence of Fe(II) and O_2. *J. Phys. Chem. A* **2024**, *128*, 10143–10150. [CrossRef]
184. Jiang, Y.-X.; Chen, Y.; Zhang, Y.-T. Modeling Study of OH Radical-Dominated H-Abstraction Reaction for Understanding Nucleotides Oxidation Induced by Cold Atmospheric Plasmas. *Plasma* **2024**, *7*, 498–509. [CrossRef]
185. Zarrouk, T.; Ibragimova, R.; Bartók, A.P.; Caro, M.A. Experiment-Driven Atomistic Materials Modeling: A Case Study Combining X-Ray Photoelectron Spectroscopy and Machine Learning Potentials to Infer the Structure of Oxygen-Rich Amorphous Carbon. *J. Am. Chem. Soc.* **2024**, *146*, 14645–14659. [CrossRef] [PubMed]
186. Kubicki, J.D.; Ohno, T. Integrating Density Functional Theory Modeling with Experimental Data to Understand and Predict Sorption Reactions: Exchange of Salicylate for Phosphate on Goethite. *Soil Syst.* **2020**, *4*, 27. [CrossRef]
187. Lowe, B.; Cardona, A.L.; Salas, J.; Bodi, A.; Mayer, P.M.; Burgos Paci, M.A. Probing the Pyrolysis of Ethyl Formate in the Dilute Gas Phase by Synchrotron Radiation and Theory. *J. Mass. Spectrom.* **2023**, *58*, e4901. [CrossRef]
188. Rossi, E.; Ciancaleoni, G. Theoretical Insights into the Reversible CO_2 Absorption by Ethylene Glycol/KOH/Boric Acid Low Temperature Transition Mixture. *J. Mol. Liq.* **2023**, *381*, 121843. [CrossRef]
189. Chandrakumar, K.R.S.; Pal, S. The Concept of Density Functional Theory Based Descriptors and Its Relation with the Reactivity of Molecular Systems: A Semi-Quantitative Study. *Int. J. Mol. Sci.* **2002**, *3*, 324–337. [CrossRef]
190. Tabti, K.; Sbai, A.; Maghat, H.; Lakhlifi, T.; Bouachrine, M. Computational Assessment of the Reactivity and Pharmaceutical Potential of Novel Triazole Derivatives: An Approach Combining DFT Calculations, Molecular Dynamics Simulations, and Molecular Docking. *Arab. J. Chem.* **2024**, *17*, 105376. [CrossRef]
191. Guan, H.; Sun, H.; Zhao, X. Application of Density Functional Theory to Molecular Engineering of Pharmaceutical Formulations. *Int. J. Mol. Sci.* **2025**, *26*, 3262. [CrossRef] [PubMed]
192. Gusarov, S. Advances in Computational Methods for Modeling Photocatalytic Reactions: A Review of Recent Developments. *Materials* **2024**, *17*, 2119. [CrossRef] [PubMed]
193. Politzer, P.; Murray, J.S. Molecular Electrostatic Potentials and Chemical Reactivity. In *Reviews in Computational Chemistry*; John Wiley & Sons, Ltd.: Hoboken, NJ, USA, 1991; pp. 273–312, ISBN 978-0-470-12579-3.
194. Politzer, P.; Murray, J.S.; Peralta-Inga, Z. Molecular Surface Electrostatic Potentials in Relation to Noncovalent Interactions in Biological Systems. *Int. J. Quantum Chem.* **2001**, *85*, 676–684. [CrossRef]
195. Sjoberg, P.; Politzer, P. Use of the Electrostatic Potential at the Molecular Surface to Interpret and Predict Nucleophilic Processes. *J. Phys. Chem.* **1990**, *94*, 3959–3961. [CrossRef]
196. Politzer, P.; Murray, J.S. The Fundamental Nature and Role of the Electrostatic Potential in Atoms and Molecules. *Theor. Chem. Acc.* **2002**, *108*, 134–142. [CrossRef]
197. Politzer, P.; Murray, J.S. Molecular Electrostatic Potentials: Significance and Applications. In *Chemical Reactivity in Confined Systems*; John Wiley & Sons, Ltd.: Hoboken, NJ, USA, 2021; pp. 113–134, ISBN 978-1-119-68335-3.
198. Murray, J.S.; Politzer, P. The Electrostatic Potential: An Overview. *WIREs Comput. Mol. Sci.* **2011**, *1*, 153–163. [CrossRef]
199. Murray, J.S.; Politzer, P. Molecular Electrostatic Potentials and Noncovalent Interactions. *WIREs Comput. Mol. Sci.* **2017**, *7*, e1326. [CrossRef]
200. Politzer, P.; Jin, P.; Murray, J.S. Atomic Polarizability, Volume and Ionization Energy. *J. Chem. Phys.* **2002**, *117*, 8197–8202. [CrossRef]
201. Politzer, P.; Murray, J.S.; Grice, M.E.; Brinck, T.; Ranganathan, S. Radial Behavior of the Average Local Ionization Energies of Atoms. *J. Chem. Phys.* **1991**, *95*, 6699–6704. [CrossRef]
202. Politzer, P.; Peralta-Inga Shields, Z.; Bulat, F.A.; Murray, J.S. Average Local Ionization Energies as a Route to Intrinsic Atomic Electronegativities. *J. Chem. Theory Comput.* **2011**, *7*, 377–384. [CrossRef] [PubMed]
203. Politzer, P.; Murray, J.S. Chapter 8 The Average Local Ionization Energy: Concepts and Applications. In *Theoretical and Computational Chemistry*; Toro-Labbé, A., Ed.; Theoretical Aspects of Chemical Reactivity; Elsevier: Amsterdam, The Netherlands, 2007; Volume 19, pp. 119–137.
204. Politzer, P.; Murray, J.S.; Bulat, F.A. Average Local Ionization Energy: A Review. *J. Mol. Model.* **2010**, *16*, 1731–1742. [CrossRef]
205. Kanagavalli, A.; Jayachitra, R.; Thilagavathi, G.; Elangovan, N.; Sowrirajan, S.; Thomas, R. Synthesis, Characterization, Computational, Excited State Properties, Wave Function, and Molecular Docking Studies of (E)-4-((2-Hydroxybenzylidene) Amino)N-(Thiazol-2-Yl) Benzenesulfonamide. *J. Indian. Chem. Soc.* **2023**, *100*, 100885. [CrossRef]
206. Rajan, M.S.; Thomas, R. Surface-Enhanced Raman Spectroscopic Sensing of the Herbicide Alachlor Using Au16 Nanocluster. *Spectrochim. Acta Part A Mol. Biomol. Spectrosc.* **2025**, *338*, 126132. [CrossRef]

207. Geethapriya, J.; Shanthidevi, A.; Arivazhagan, M.; Elangovan, N.; Sowrirajan, S.; Manivel, S.; Thomas, R. Synthesis, Characterization, Computational, Excited State Properties, Wave Function and Molecular Docking Studies of (E)-1-(Perfluorophenyl)-N-(p-Tolyl) Methanimine. *J. Indian. Chem. Soc.* **2022**, *99*, 100785. [CrossRef]
208. Isravel, A.D.; Jeyaraj, J.K.; Thangasamy, S.; John, W.J. DFT, NBO, HOMO-LUMO, NCI, Stability, Fukui Function and Hole—Electron Analyses of Tolcapone. *Comput. Theor. Chem.* **2021**, *1202*, 113296. [CrossRef]
209. Bultinck, P.; Winter, H.D.; Langenaeker, W.; Tollenare, J.P. *Computational Medicinal Chemistry for Drug Discovery*; CRC Press: Boca Raton, FL, USA, 2003; ISBN 978-0-203-91339-0.
210. Pal, R.; Chattaraj, P.K. Chemical Reactivity from a Conceptual Density Functional Theory Perspective. *J. Indian. Chem. Soc.* **2021**, *98*, 100008. [CrossRef]
211. Rincón, L.; Rodríguez, W.M.; Mora, J.R.; Zambrano, C.; Seijas, L.E.; Reyes, A.; Torres, F.J. A Redefinition of Global Conceptual Density Functional Theory Reactivity Indexes by Means of the Cubic Expansions of the Energy. *Phys. Chem. Chem. Phys.* **2025**, *27*, 8174–8185. [CrossRef]
212. Bhatia, M. An Overview of Conceptual-DFT Based Insights into Global Chemical Reactivity of Volatile Sulfur Compounds (VSCs). *Comput. Toxicol.* **2024**, *29*, 100295. [CrossRef]
213. Ramírez-Martínez, C.; Zárate-Hernández, L.A.; Camacho-Mendoza, R.L.; González-Montiel, S.; Meneses-Viveros, A.; Cruz-Borbolla, J. The Use of Global and Local Reactivity Descriptors of Conceptual DFT to Describe Toxicity of Benzoic Acid Derivatives. *Comput. Theor. Chem.* **2023**, *1226*, 114211. [CrossRef]
214. Wang, S.; Hao, C.; Gao, Z.; Chen, J.; Qiu, J. Theoretical Investigation on Photodechlorination Mechanism of Polychlorinated Biphenyls. *Chemosphere* **2014**, *95*, 200–205. [CrossRef]
215. Armaković, S.; Armaković, S.J.; Abramović, B.F. Theoretical Investigation of Loratadine Reactivity in Order to Understand Its Degradation Properties: DFT and MD Study. *J. Mol. Model.* **2016**, *22*, 240. [CrossRef] [PubMed]
216. Case, D.A.; Aktulga, H.M.; Belfon, K.; Cerutti, D.S.; Cisneros, G.A.; Cruzeiro, V.W.D.; Forouzesh, N.; Giese, T.J.; Götz, A.W.; Gohlke, H.; et al. AmberTools. *J. Chem. Inf. Model.* **2023**, *63*, 6183–6191. [CrossRef]
217. MacKerell, A.D., Jr.; Brooks, B.; Brooks, C.L., III; Nilsson, L.; Roux, B.; Won, Y.; Karplus, M. CHARMM: The Energy Function and Its Parameterization. In *Encyclopedia of Computational Chemistry*; John Wiley & Sons, Ltd.: Hoboken, NJ, USA, 2002; ISBN 978-0-470-84501-1.
218. Brooks, B.R.; Bruccoleri, R.E.; Olafson, B.D.; States, D.J.; Swaminathan, S.; Karplus, M. CHARMM: A Program for Macromolecular Energy, Minimization, and Dynamics Calculations. *J. Comput. Chem.* **1983**, *4*, 187–217. [CrossRef]
219. Brooks, B.R.; Brooks, C.L.; MacKerell, A.D.; Nilsson, L.; Petrella, R.J.; Roux, B.; Won, Y.; Archontis, G.; Bartels, C.; Boresch, S.; et al. CHARMM: The Biomolecular Simulation Program. *J. Comput. Chem.* **2009**, *30*, 1545–1614. [CrossRef] [PubMed]
220. Jorgensen, W.L.; Tirado-Rives, J. The OPLS [Optimized Potentials for Liquid Simulations] Potential Functions for Proteins, Energy Minimizations for Crystals of Cyclic Peptides and Crambin. *J. Am. Chem. Soc.* **1988**, *110*, 1657–1666. [CrossRef]
221. Jorgensen, W.L.; Maxwell, D.S.; Tirado-Rives, J. Development and Testing of the OPLS All-Atom Force Field on Conformational Energetics and Properties of Organic Liquids. *J. Am. Chem. Soc.* **1996**, *118*, 11225–11236. [CrossRef]
222. Shivakumar, D.; Williams, J.; Wu, Y.; Damm, W.; Shelley, J.; Sherman, W. Prediction of Absolute Solvation Free Energies Using Molecular Dynamics Free Energy Perturbation and the OPLS Force Field. *J. Chem. Theory Comput.* **2010**, *6*, 1509–1519. [CrossRef] [PubMed]
223. Harder, E.; Damm, W.; Maple, J.; Wu, C.; Reboul, M.; Xiang, J.Y.; Wang, L.; Lupyan, D.; Dahlgren, M.K.; Knight, J.L.; et al. OPLS3: A Force Field Providing Broad Coverage of Drug-like Small Molecules and Proteins. *J. Chem. Theory Comput.* **2016**, *12*, 281–296. [CrossRef]
224. Roos, K.; Wu, C.; Damm, W.; Reboul, M.; Stevenson, J.M.; Lu, C.; Dahlgren, M.K.; Mondal, S.; Chen, W.; Wang, L.; et al. OPLS3e: Extending Force Field Coverage for Drug-Like Small Molecules. *J. Chem. Theory Comput.* **2019**, *15*, 1863–1874. [CrossRef]
225. Lu, C.; Wu, C.; Ghoreishi, D.; Chen, W.; Wang, L.; Damm, W.; Ross, G.A.; Dahlgren, M.K.; Russell, E.; Von Bargen, C.D.; et al. OPLS4: Improving Force Field Accuracy on Challenging Regimes of Chemical Space. *J. Chem. Theory Comput.* **2021**, *17*, 4291–4300. [CrossRef]
226. Dixon, T.; MacPherson, D.; Mostofian, B.; Dauzhenka, T.; Lotz, S.; McGee, D.; Shechter, S.; Shrestha, U.R.; Wiewiora, R.; McDargh, Z.A.; et al. Predicting the Structural Basis of Targeted Protein Degradation by Integrating Molecular Dynamics Simulations with Structural Mass Spectrometry. *Nat. Commun.* **2022**, *13*, 5884. [CrossRef]
227. Wales, D.J.; Doye, J.P.K. Global Optimization by Basin-Hopping and the Lowest Energy Structures of Lennard-Jones Clusters Containing up to 110 Atoms. *J. Phys. Chem. A* **1997**, *101*, 5111–5116. [CrossRef]
228. Goedecker, S. Minima Hopping: An Efficient Search Method for the Global Minimum of the Potential Energy Surface of Complex Molecular Systems. *J. Chem. Phys.* **2004**, *120*, 9911–9917. [CrossRef]
229. de Souza, B. GOAT: A Global Optimization Algorithm for Molecules and Atomic Clusters. *Angew. Chem. Int. Ed.* **2025**, *64*, e202500393. [CrossRef]

230. Wesołowski, P.A.; Wales, D.J.; Pracht, P. Multilevel Framework for Analysis of Protein Folding Involving Disulfide Bond Formation. *J. Phys. Chem. B* **2024**, *128*, 3145–3156. [CrossRef] [PubMed]
231. Pracht, P.; Bannwarth, C. Fast Screening of Minimum Energy Crossing Points with Semiempirical Tight-Binding Methods. *J. Chem. Theory Comput.* **2022**, *18*, 6370–6385. [CrossRef]
232. Spicher, S.; Plett, C.; Pracht, P.; Hansen, A.; Grimme, S. Automated Molecular Cluster Growing for Explicit Solvation by Efficient Force Field and Tight Binding Methods. *J. Chem. Theory Comput.* **2022**, *18*, 3174–3189. [CrossRef]
233. Pracht, P.; Bauer, C.A.; Grimme, S. Automated and Efficient Quantum Chemical Determination and Energetic Ranking of Molecular Protonation Sites. *J. Comput. Chem.* **2017**, *38*, 2618–2631. [CrossRef] [PubMed]
234. Grimme, S. Exploration of Chemical Compound, Conformer, and Reaction Space with Meta-Dynamics Simulations Based on Tight-Binding Quantum Chemical Calculations. *J. Chem. Theory Comput.* **2019**, *15*, 2847–2862. [CrossRef]
235. Pracht, P.; Grimme, S. Calculation of Absolute Molecular Entropies and Heat Capacities Made Simple. *Chem. Sci.* **2021**, *12*, 6551–6568. [CrossRef]
236. Pracht, P.; Grimme, S.; Bannwarth, C.; Bohle, F.; Ehlert, S.; Feldmann, G.; Gorges, J.; Müller, M.; Neudecker, T.; Plett, C.; et al. CREST—A Program for the Exploration of Low-Energy Molecular Chemical Space. *J. Chem. Phys.* **2024**, *160*, 114110. [CrossRef]
237. Koopman, J.; Grimme, S. Calculation of Mass Spectra with the QC × MS Method for Negatively and Multiply Charged Molecules. *J. Am. Soc. Mass Spectrom.* **2022**, *33*, 2226–2242. [CrossRef]
238. Schnegotzki, R.; Koopman, J.; Grimme, S.; Süssmuth, R.D. Quantum Chemistry-Based Molecular Dynamics Simulations as a Tool for the Assignment of ESI-MS/MS Spectra of Drug Molecules. *Chem.—A Eur. J.* **2022**, *28*, e202200318. [CrossRef]
239. Schreckenbach, S.A.; Anderson, J.S.M.; Koopman, J.; Grimme, S.; Simpson, M.J.; Jobst, K.J. Predicting the Mass Spectra of Environmental Pollutants Using Computational Chemistry: A Case Study and Critical Evaluation. *J. Am. Soc. Mass. Spectrom.* **2021**, *32*, 1508–1518. [CrossRef] [PubMed]
240. Koopman, J.; Grimme, S. From QCEIMS to QCxMS: A Tool to Routinely Calculate CID Mass Spectra Using Molecular Dynamics. *J. Am. Soc. Mass. Spectrom.* **2021**, *32*, 1735–1751. [CrossRef] [PubMed]
241. Ásgeirsson, V.; Bauer, C.A.; Grimme, S. Unimolecular Decomposition Pathways of Negatively Charged Nitriles by Ab Initio Molecular Dynamics. *Phys. Chem. Chem. Phys.* **2016**, *18*, 31017–31026. [CrossRef] [PubMed]
242. Koopman, J.; Grimme, S. Calculation of Electron Ionization Mass Spectra with Semiempirical GFNn-xTB Methods. *ACS Omega* **2019**, *4*, 15120–15133. [CrossRef] [PubMed]
243. Ásgeirsson, V.; Bauer, C.A.; Grimme, S. Quantum Chemical Calculation of Electron Ionization Mass Spectra for General Organic and Inorganic Molecules. *Chem. Sci.* **2017**, *8*, 4879–4895. [CrossRef] [PubMed]
244. Bauer, C.A.; Grimme, S. How to Compute Electron Ionization Mass Spectra from First Principles. *J. Phys. Chem. A* **2016**, *120*, 3755–3766. [CrossRef]
245. Bauer, C.A.; Grimme, S. Automated Quantum Chemistry Based Molecular Dynamics Simulations of Electron Ionization Induced Fragmentations of the Nucleobases Uracil, Thymine, Cytosine, and Guanine. *Eur. J. Mass Spectrom. (Chichester)* **2015**, *21*, 125–140. [CrossRef]
246. Bauer, C.A.; Grimme, S. Elucidation of Electron Ionization Induced Fragmentations of Adenine by Semiempirical and Density Functional Molecular Dynamics. *J. Phys. Chem. A* **2014**, *118*, 11479–11484. [CrossRef]
247. Bauer, C.A.; Grimme, S. First Principles Calculation of Electron Ionization Mass Spectra for Selected Organic Drug Molecules. *Org. Biomol. Chem.* **2014**, *12*, 8737–8744. [CrossRef]
248. Grimme, S. Towards First Principles Calculation of Electron Impact Mass Spectra of Molecules. *Angew. Chem. Int. Ed.* **2013**, *52*, 6306–6312. [CrossRef]
249. Gorges, J.; Grimme, S. QC × MS2—A Program for the Calculation of Electron Ionization Mass Spectra via Automated Reaction Network Discovery. *Phys. Chem. Chem. Phys.* **2025**, *27*, 6899–6911. [CrossRef]